This is to certify that the
thesis entitled

ION-EXCHANGE MEMBRANES PREPARED USING LAYER-BY-LAYER POLYELECTROLYTE DEPOSITION

presented by

GUANQING LIU

has been accepted towards fulfillment
of the requirements for the

M.S. degree in Chemistry

Major Professor's Signature

10/28/2009

Date

ION-EXCHANGE MEMBRANES PREPARED USING LAYER-BY-LAYER POLYELECTROLYTE DEPOSITION

By

Guanqing Liu

A THESIS

Submitted to
Michigan State University
in partial fulfillment of the requirements
for the degree of

MASTERS OF SCIENCE

Chemistry

2009

ABSTRACT

ION-EXCHANGE MEMBRANES PREPARED USING LAYER-BY-LAYER POLYELECTROLYTE DEPOSITION

By

Guanqing Liu

Layer-by-layer polyelectrolyte adsorption in porous polymeric membranes provides a simple way to create ion-exchange sites without greatly decreasing hydraulic permeability (<20% reduction in permeability). At 80% breakthrough, membranes coated with 3-bilayer poly(styrene sulfonate) (PSS)/polyethyleneimine (PEI) films bind 37±6 mg of negatively charged Au colloids per mL of membrane volume. The binding capacity of membranes coated with 1-bilayer films decreases in the order PSS/PEI>PSS/poly(diallyldimethyl ammonium chloride)>PSS/poly(allylamine). Films terminated with a polyanion present cation-exchange sites that bind lysozyme, and the lysozyme-binding capacities of $(PSS/PEI)_3$/PSS films increase with the ionic strength of the solution from which the last PSS layer is deposited. Charge screening during deposition of the terminal PSS layer likely gives rise to a larger number of ion-exchange sites and lysozyme-binding capacities as high as 16 mg/mL. At 10% breakthrough, a stack of 3 membranes binds 3 times as much lysozyme as a single membrane, showing that stacking is an effective way to increase capacity.

To my father, Deyu Liu and my mother, Runlan Mei

ACKNOWLEDGEMENTS

In the first place, I would like to thank my advisor, Professor Merlin Bruening, for all his kindness and help throughout the past two years. He is such a nice person that instructions from him bring me a large part of my initiative and motivation. He has offered guidelines, not only for the solutions to experiments, but also for the way of thinking as a scientist. I appreciate his patience when things were stuck, his tolerance when things were messing up, and his encouragement when things were working out.

I would also like to express my gratitude and appreciation to past and present members in the Bruening group for their help and suggestions in the last two years. I am especially grateful to Dr. Parul Jain, Dr. Weihan Wang, and Dr. David Dotzauer for their direct involvement in my research projects and their instructions on the operation of certain experiments and instruments. I'd like to thank the other personnel with whom I have being working as well. I had a great time in the lab with all you guys.

I want to thank Dr. Daniel Jones, Dr. Jetze Tepe, and Dr. Dana Spence for joining my guidance committee and providing great help. I'd like to show my appreciation to the National Science Foundation for funding my research and Michigan State University for providing me such a wonderful study experience.

Last, but not least, I would like to give all my appreciation and thankfulness to my family and friends, for their great, continuous, and permanent support and understanding.

TABLE OF CONTENTS

LIST OF TABLES

LIST OF FIGURES

LIST OF ABBREVIATIONS

ATR	attenuated total reflection
ATRP	atom transfer radical polymerization
BSA	bovine serum albumin
DNA	deoxyribonucleic acid
FTIR	Fourier transform infrared
LBL	layer-by-layer
PAA	poly(acrylic acid)
PAH	poly(allylamine hydrochloride)
PDADMAC	poly(diallyldimethylammonium chloride)
PEI	poly(ethyleneimine)
PES	polyethersulfone
pI	isoelectric point
PMMA	poly(methyl methacrylate)
PSS	poly(sodium 4-styrenesulfonate)
PVDF	polyvinylidene chloride
RC	regenerated cellulose
SEM	scanning electron microscopy
UV-Vis	ultraviolet-visible
ζ	zeta potential

Chapter 1

Introduction and Background

1.1 Background

This thesis describes a new method for creating ion-exchange membranes and investigations of these membranes as absorbers of nanoparticles and proteins. To put this work in perspective, I first compare membrane absorbers with chromatographic separations of proteins and small molecules.

1.1.1 Chromatographic Separations

Separations have always been a primary task for analytical chemists. According to the Second Law of Thermodynamics, the entropy of any isolated system tends to increase for spontaneous processes.[1] In contrast, separations, which transform a mixture of substances into two or more distinct products, require a decline in system entropy and an input of external energy.

Column chromatography is one of the most powerful separation techniques, and packed columns have been the primary tools for protein separation and analysis for several decades. In a typical separation (Figure 1.1), a column packed with stationary phase is equilibrated with the mobile phase, and after application of the sample to the column, the flow of mobile phase separates components of the sample into specific bands.[2] The process may take from minutes to days, depending on the type of samples and the length of the column.

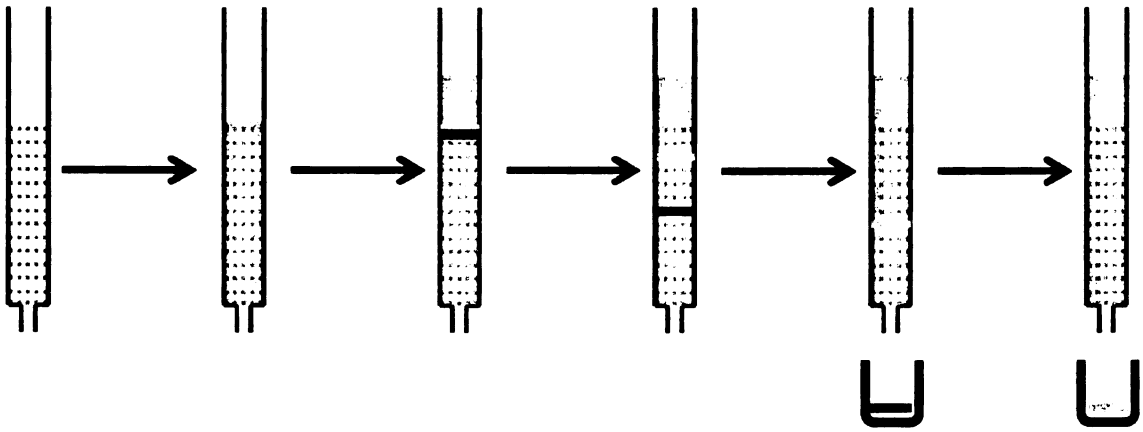

Figure 1.1: Column chromatography.

Column chromatography has many assets such as ease of operation, applicability to a wide range of analytes, and compatibility with a number of detectors. However, it also suffers several limitations.[3-7] First, due to the compact stationary phase, the pressure drop across the packed bed is generally high. Second, in high capacity separation of proteins, adsorption includes intra-particle diffusive transport of the proteins to the binding sites within the bead pores (Figure 1.2a). As a result, the speed and throughput of packed-bed separations are relatively low. Furthermore, the eluent volume is relatively large, so solvent consumption and analyte dilution can be a problem.

Miniaturization of columns may decrease solvent consumption and analysis time, but this is not a viable solution for preparative separations.[8] Over the last few years, porous monolithic stationary phases have been developed to overcome some diffusion limitations.[9] However, these media are expensive, and their capacity is relatively low since they do not contain nanopores with high surface area.

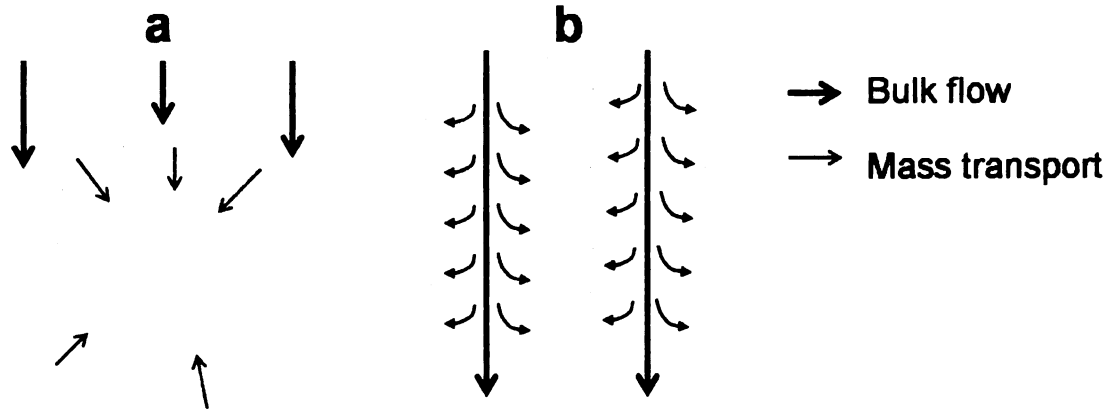

Figure 1.2: Solute transport in (a) the beads of a packed column and (b) the pores of a membrane. In (a), separation is limited by the transport of solutes into and out of the pores of beads, whereas transport occurs by convection in (b).

1.1.2 Membrane Absorbers as an Alternative Platform for Protein Separation

Membrane absorbers utilize microporous and macroporous membranes modified with functional ligands, and their application to protein separation and purification provides an alternative approach to packed-bed chromatography.[10] In principle, membrane absorbers offer the follow advantages relative to packed columns: 1) the transport of solutes to the binding sites in membranes occurs by convection instead of diffusion (Figure 1.2b), which accelerates the separation process; 2) the short flow path across the membrane results in a low pressure drop; 3) the pore size of the membranes can be as large as a few microns so that larger proteins, which do not enter the nanopores of packed beads, can still bind to the membranes; 4) the easy packing and scale-up of membranes may accommodate high-productivity applications; and 5) the low price for mass production makes it possible to develop disposable membrane absorbers with desired functionalities.[5, 11-13]

Membrane systems are available in distinct geometries such as flat-sheets,[5] hollow fibers,[14] and spiral-wound[15] modules. Among all these module types, flat-sheet membranes are the most commonly studied because they are most easily characterized.

Typical binding mechanisms employed in membrane absorbers include ion-exchange, affinity binding, and hydrophobic interactions.[3] However, in the application of membrane absorbers for protein separations, ion exchange constitutes almost half of the commercial market[5], because it is applicable to a wide range of proteins and does not require specific tags. (Essentially all proteins are charge at certain pH values.) This work focuses on developing simple, inexpensive methods for modifying membranes with ion-exchange sites, and the following section discusses ion-exchange membrane absorbers in more detail.

1.1.3 Ion-Exchange Membrane Absorbers for Protein Separation

Ion-exchange membrane absorbers take advantage of electrostatic interactions between the analyte of interest and charged membrane pores to facilitate separation and purification. The net charge of proteins varies with both the amino acid sequence and the solution pH, and differences in net charge at a given pH allow selective retention of specific proteins in ion-exchange membranes. Elution with highly concentrated buffer disrupts electrostatic interactions to facilitate protein recovery (Figure 1.3).

Lysozyme and BSA are the most common test proteins employed to examine the performance of ion-exchange membranes in protein separations. The isoelectric points of these proteins are 10.7 and 4.8, respectively, so at neutral pH, lysozyme is positively

charged and BSA is negatively charged. Husson's group used BSA to test the binding performance of their weak anion-exchange membranes,[4, 16] whereas Ulbricht and colleagues employed lysozyme for examination of their cation-exchange membrane adsorbers.[17]

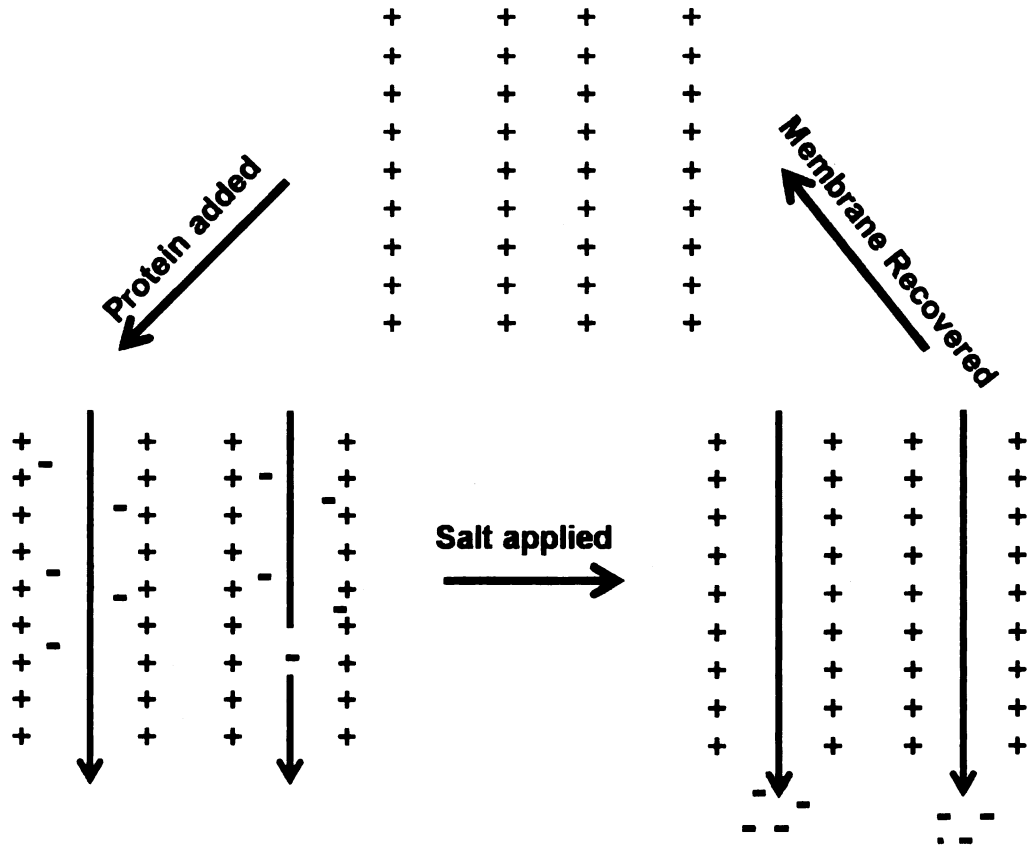

Figure 1.3: Ion-exchange membrane separations. The "+" signs represent the charges inside the membrane pores, and negatively charged spheres are the analyte of interest. The arrows in the membrane show the flow direction during the separation process.

1.2 Preparation of Ion-Exchange Membranes

A number of porous inorganic and polymeric substrates can serves as membrane absorbers, but they typically have limited functionality. Thus, modification of porous

membranes to generate selective adsorptive sites is vital to exploit the potential of these substrates. Several groups worked on extending the binding capacities and selectivity of ion-exchange membranes by introducing functional polymers. Graft polymerization, including radiation grafting,[18, 19] photografting,[20-22] and atom transfer radial polymerization (ATRP) from immobilized initiators[7, 16] offer ways to build high density ion-exchange polymers in porous substrates. Regenerated cellulose (RC),[23, 24] polyethylene,[25, 26] polyvinylidene difluoride (PVDF),[27] polyethersulfone (PES),[28] nylon,[29] and polypropylene[18] have been modified with grafted polymers to generate membrane absorbers. This work aims to develop a simpler method, layer-by-layer adsorption of polyelectrolytes, to create ion-exchange membranes.

1.3 Layer-by-Layer (LBL) Deposition of Polyelectrolyte Films

Decher and coworkers first introduced layer-by-layer (LBL) adsorption of polyelectrolytes to construct multilayer polymer films in the 1990s.[30, 31] Figure 1.4 outlines the LBL procedure.[32] Generally, the process begins with immersion of a charged substrate in a solution containing a polyelectrolyte with the opposite charge of the substrate surface. After allowing time for polyelectrolyte adsorption, rinsing of the modified substrate removes physically adsorbed polyions. Immersion into a solution containing a second polyelectrolyte, with opposite charge to the first polyelectrolyte, results in adsorption of a second "layer", and repetition of the process allows deposition of the desired number of polyelectrolyte layers. The thickness of the multilayered polyelectrolytes is a function of several parameters, including the concentration of

polyelectrolyte in solution, adsorption time, the ionic strength of the deposition solutions, solvent composition, and temperature.[33]

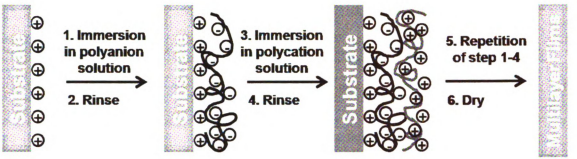

Figure 1.4: Formation of multilayer polyelectrolyte films through LBL deposition.

This deposition process relies on electrostatic interactions between the charged surface and polyelectrolytes, however, the driving force for film formation is an increase in entropy.[34] Upon polyelectrolyte adsorption, the requirement of electrical neutrality induces the release of a large number of ions that were associated with the previous polyelectrolyte layer and the polyelectrolyte that was adsorbed. The entropy gained in the release of large quantities of ions drives the spontaneous deposition of polymer films.

A large number of charged substrates can serve as the templates for the growth of polyelectrolyte films. Au, silica, and mica are typical surfaces for LBL deposition, and macroporous membranes[35, 36] and natural fibers[37] can also be coated with these films. The rapid development of potential applications of the LBL technique stems from the following assets of this film-deposition method:[38] 1) the process for film construction occurs with a simple "dip and rinse" method that is very convenient in the laboratory; 2) the properties of the multilayered films can be manipulated by varying factors such as pH and ionic strength;[39-42] 3) nearly any multiply charged species can serve as a film

constituent, which allows for a great diversity of film properties; and 4) the large number of available substrates for LBL deposition lead to a vast scope of possible applications.

1.4 LBL Modification of Membranes for Nanofiltration and Catalysis

LBL deposition techniques are attractive for a large number of applications including the fabrication of nanofiltration membranes.[43] Multilayer polyelectrolyte films are attractive as the selective skins of nanofiltration membranes because: 1) the construction of polyelectrolyte films on membrane substrates is a simple process; 2) film thickness can be well controlled at the nanometer scale to ensure high flux; and 3) film properties are adjustable through variation of polyelectrolytes or deposition conditions.[40, 44-46] Ouyang *et al.* modified porous alumina membranes with poly(styrene sulfonate) (PSS)/poly(allylamine) (PAH) and PSS/poly(diallyldimethyl ammonium chloride) (PDADMAC) for the separation of Na^+ and Ca^{2+} as well as Na^+ and Mg^{2+}.[47]

Another promising application of polyelectrolyte multilayers is the preparation of catalytic membranes. Dotzauer *et al.* deposited poly(acrylic acid) (PAA)/PAH films into porous alumina membranes prior to the immobilization of Au nanoparticles.[48] The membranes showed extremely high conversion (>99%) in the reduction of 4-nitrophenol to 4-aminophenol. Other substrates such as nylon and polycarbonate membranes can also be modified to catalyze reduction of a number of nitroaromatic compounds.[49] This work examines the filtration and capture of nanoparticles using polyelectrolyte-modified membranes.

1.5 Research Motivation and Objectives

The objective of this thesis is to develop a simple method to form ion-exchange membranes through LBL deposition of polyelectrolyte multilayers. Several groups deposited LBL films on the top of porous ultrafiltration materials to create composite membranes, but such systems are designed primarily for size-based or charge-based separation of small molecules.[50-55] Two other studies demonstrated fabrication of polyelectrolyte nanotubes in porous alumina membranes.[35, 36] In that case, the porous membrane serves as a template for the preparation of multilayer films, and dissolution of the membrane yields the nanotubes. More recently, polyelectrolyte-modified membranes served as substrates for enzymes,[56] nanoparticle catalysts,[48] and protein arrays.[57]

This research shows that porous membranes modified with LBL polyelectrolyte films are effective ion-exchange membranes for removal of Au nanoparticles and proteins from solution (see Figure 1.5). The films adsorb in a variety of membranes without greatly decreasing membrane permeability. The research compares the adsorption capacities of films prepared with two polyanions, PSS and PAA, and three polycations, protonated polyethyleneimine (PEI), protonated PAH, and PDADMAC. We also examine several polymeric substrates including nylon, PES, and PVDF membranes with 5 μm nominal pore size and RC membranes with 1 μm nominal pore size. The best membranes have a Au-nanoparticle binding capacity of 37±6 mg/mL and a lysozyme binding capacity of 16 mg/mL. Importantly, the high permeability of the modified substrates allows for the use of membrane stacks that exhibit low pressure drops, and the amount of protein adsorbed is proportional to the number of membranes in the stack.

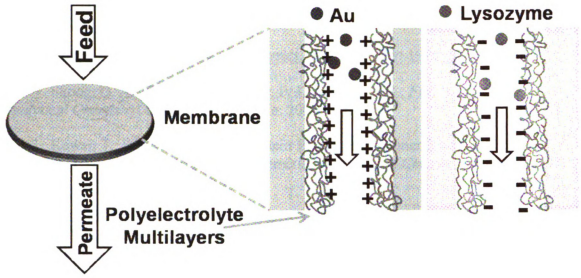

Figure 1.5: Schematic diagram showing the binding of negatively charged Au nanoparticles (left) and positively charged lysozyme (right) to polyelectrolyte-multilayer-modified membranes terminated with a polycation (left) and a polyanion (right).

1.6 References

1. Cutnell, J. D.; Johnson, K. W., *Physics*. 3rd ed.; Wiley: 1995; p 470.

2. Skoog, D. A.; West, D. M.; Holler, F. J.; Crouch, S. R., *Fundamentals of Analytical Chemistry*. 8th ed.; Brooks/Cole: 2004; p 973.

3. Kawai, T.; Saito, K.; Lee, W., Protein Binding to Polymer Brush, Based on Ion-Exchange, Hydrophobic, and Affinity Interactions. *Journal of Chromatography B* **2003,** 790, (1-2), 131-142.

4. Bhut, B. V.; Husson, S. M., Dramatic Performance Improvement of Weak Anion-Exchange Membranes for Chromatographic Bioseparations. *Journal of Membrane Science* **2009,** 337, (1-2), 215-223.

5. Ghosh, R., Protein Separation Using Membrane Chromatography: Opportunities and Challenges. *Journal of Chromatography A* **2002,** 952, (1-2), 13-27.

6. Ghosh, R., Separation of Proteins Using Hydrophobic Interaction Membrane Chromatography. *Journal of Chromatography A* **2001,** 923, (1-2), 59-64.

7. Singh, N.; Wang, J.; Ulbricht, M.; Wickramasinghe, S. R.; Husson, S. M., Surface-Initiated Atom Transfer Radical Polymerization: A New Method for Preparation of Polymeric Membrane Adsorbers. *Journal of Membrane Science* **2008,** 309, (1-2), 64-72.

8. Dittrich, P. S.; Tachikawa, K.; Manz, A., Micro Total Analysis Systems. Latest Advancements and Trends. *Analytical Chemistry* **2006,** 78, (12), 3887-3908.

9. Alois, J.; Rainer, H., Monoliths for Fast Bioseparation and Bioconversion and their Applications in Biotechnology. *Journal of Separation Science* **2004,** 27, (10-11), 767-778.

10. Saxena, A.; Tripathi, B. P.; Kumar, M.; Shahi, V. K., Membrane-Based Techniques for the Separation and Purification of Proteins: An Overview. *Advances in Colloid and Interface Science* **2009,** 145, (1-2), 1-22.

11. Knudsen, H. L.; Fahrner, R. L.; Xu, Y.; Norling, L. A.; Blank, G. S., Membrane Ion-Exchange Chromatography for Process-Scale Antibody Purification. *Journal of Chromatography A* **2001,** 907, (1-2), 145-154.

12. Lightfoot, E. N.; Moscariello, J. S., Bioseparations. *Biotechnology and Bioengineering* **2004,** 87, (3), 259-273.

13. Jorg, T.; Mark, E., Alternatives to Chromatographic Separations. *Biotechnology Progress* **2007,** 23, (1), 42-45.

14. van Reis, R.; Zydney, A., Bioprocess Membrane Technology. *Journal of Membrane Science* **2007,** 297, (1-2), 16-50.

15. Finger, U. B.; Thomes, J.; Kinzelt, D.; Kula, M. R., Application of Thiophilic Membranes for the Purification of Monoclonal Antibodies from Cell Culture Media. *Journal of Chromatography B: Biomedical Sciences and Applications* **1995,** 664, (1), 69-78.

16. Bhut, B. V.; Wickramasinghe, S. R.; Husson, S. M., Preparation of High-Capacity, Weak Anion-Exchange Membranes for Protein Separations Using Surface-Initiated Atom Transfer Radical Polymerization. *Journal of Membrane Science* **2008,** 325, (1), 176-183.

17. Mohd Yusof, A. H.; Ulbricht, M., Polypropylene-Based Membrane Adsorbers via Photo-Initiated Graft Copolymerization: Optimizing Separation Performance by Preparation Conditions. *Journal of Membrane Science* **2008,** 311, (1-2), 294-305.

18. Kobayashi, K.; Tsuneda, S.; Saito, K.; Yamagishi, H.; Furusaki, S.; Sugo, T., Preparation of Microfiltration Membranes Containing Anion-Exchange Groups. *Journal of Membrane Science* **1993,** 76, (2-3), 209-218.

19. Virendra, K.; Bhardwaj, Y. K.; Jamdar, S. N.; Goel, N. K.; Sabharwal, S., Preparation of an Anion-Exchange Adsorbent by the Radiation-Induced Grafting of Vinylbenzyltrimethylammonium Chloride onto Cotton Cellulose and its Application for Protein Adsorption. *Journal of Applied Polymer Science* **2006,** 102, (6), 5512-5521.

20. Kacar, Y.; Arica, M. Y., Procion Green H-E4BD-Immobilized Porous Poly(Hydroxyethylmethacrylate) Ion-Exchange Membrane: Preparation and Application to Lysozyme Adsorption. *Colloids and Surfaces B: Biointerfaces* **2001,** 22, (3), 227-236.

21. Ulbricht, M.; Yang, H., Porous Polypropylene Membranes with Different Carboxyl Polymer Brush Layers for Reversible Protein Binding via Surface-Initiated Graft Copolymerization. *Chemistry of Materials* **2005,** 17, (10), 2622-2631.

22. Yusof, A. H. M.; Ulbricht, M., Effects of Photo-Initiation and Monomer Composition onto Performance of Graft-Copolymer Based Membrane Adsorbers. *Desalination* **2006,** 200, (1-3), 462-463.

23. Guo, W.; Ruckenstein, E., A New Matrix for Membrane Affinity Chromatography and its Application to the Purification of Concanavalin A. *Journal of Membrane Science* **2001,** 182, (1-2), 227-234.

24. Francesca, C.; Giulio, C. S., Separation of MBP Fusion Proteins through Affinity Membranes. *Biotechnology Progress* **2002,** 18, (1), 94-100.

25. Kim, M.; Saito, K.; Furusaki, S.; Sugo, T.; Ishigaki, I., Protein Adsorption Capacity of a Porous Phenylalanine-Containing Membrane Based on a Polyethylene Matrix. *Journal of Chromatography A* **1991,** 586, (1), 27-33.

26. Noboru, K.; Minoru, K.; Kyoichi, S.; Kazuyuki, S.; Kohei, W.; Takanobu, S., Protein Adsorption and Elution Performances of Porous Hollow-Fiber Membranes Containing Various Hydrophobic Ligands. *Biotechnology Progress* **1997,** 13, (1), 89-95.

27. Singh, N.; Husson, S. M.; Zdyrko, B.; Luzinov, I., Surface Modification of Microporous PVDF Membranes by ATRP. *Journal of Membrane Science* **2005,** 262, (1-2), 81-90.

28. Catherine, C.; Zhiguo, S.; Sujatha, K.; Gregor, D.; Clark, K. C., Protein A Immunoaffinity Hollow Fiber Membranes for Immunoglobulin G Purification: Experimental Characterization. *Biotechnology and Bioengineering* **1995,** 48, (4), 415-427.

29. Castilho, L. R.; Deckwer, W. D.; Anspach, F. B., Influence of Matrix Activation and Polymer Coating on the Purification of Human IgG with Protein A Affinity Membranes. *Journal of Membrane Science* **2000,** 172, (1-2), 269-277.

30. Decher, G.; Hong, J. D., Buildup of Ultrathin Multilayer Films by a Self-Assembly Process. 1. Consecutive Adsorption of Anionic and Cationic Bipolar Amphiphiles on Charged Surfaces. *Makromolekulare Chemie-Macromolecular Symposia* **1991,** 46, 321-327.

31. Decher, G.; Hong, J. D., Buildup of Ultrathin Multilayer Films by a Self-Assembly Process. 2. Consecutive Adsorption of Anionic and Cationic Bipolar Amphiphiles and Polyelectrolytes on Charged Surfaces. *Berichte der Bunsen-Gesellschaft Physical Chemistry Chemical Physics* **1991,** 95, (11), 1430-1434.

32. Decher, G., Fuzzy Nanoassemblies: Toward Layered Polymeric Multicomposites. *Science* **1997,** 277, (5330), 1232-1237.

33. Decher, G., Polyelectrolyte Multilayers, an Overview. In *Multilayer Thin Films*, Gero Decher, J. B. S., Ed. Wiley: 2003; p 6.

34. Arys, X.; Jonas, A. M.; Laschewsky, A.; Legras, R., *Supramolecular Polymers*. CRC Press: New York, 2000.

35. Liang, Z.; Susha, A. S.; Yu, A.; Caruso, F., Nanotubes Prepared by Layer-by-Layer Coating of Porous Membrane Templates. *Advanced Materials* **2003,** 15, (21), 1849-1853.

36. Ai, S.; Lu, G.; He, Q.; Li, J., Highly Flexible Polyelectrolyte Nanotubes. *Journal of the American Chemical Society* **2003,** 125, (37), 11140-11141.

37. Kevin, H.; Mariana, R.; Juan, H., Layer-by-Layer Deposition of Polyelectrolyte Nanolayers on Natural Fibres: Cotton. *Nanotechnology* **2005,** (7), S422.

38. Dai, J. Application of Multilayer Polyelectrolyte Films in Corrosion Inhibition, Ion Separation, and Catalysis. Ph.D Thesis, Michigan State University, East Lansing, 2002.

39. Caruso, F.; Niikura, K.; Furlong, D. N.; Okahata, Y., 1. Ultrathin Multilayer Polyelectrolyte Films on Gold: Construction and Thickness Determination. *Langmuir* **1997,** 13, (13), 3422-3426.

40. Yoo, D.; Shiratori, S. S.; Rubner, M. F., Controlling Bilayer Composition and Surface Wettability of Sequentially Adsorbed Multilayers of Weak Polyelectrolytes. *Macromolecules* **1998,** 31, (13), 4309-4318.

41. Dubas, S. T.; Schlenoff, J. B., Factors Controlling the Growth of Polyelectrolyte Multilayers. *Macromolecules* **1999,** 32, (24), 8153-8160.

42. Harris, J. J.; Bruening, M. L., Electrochemical and in Situ Ellipsometric Investigation of the Permeability and Stability of Layered Polyelectrolyte Films. *Langmuir* **1999,** 16, (4), 2006-2013.

43. Harris, J. J.; Stair, J. L.; Bruening, M. L., Layered Polyelectrolyte Films as Selective, Ultrathin Barriers for Anion Transport. *Chemistry of Materials* **2000,** 12, (7), 1941-1946.

44. Lõsche, M.; Schmitt, J.; Decher, G.; Bouwman, W. G.; Kjaer, K., Detailed Structure of Molecularly Thin Polyelectrolyte Multilayer Films on Solid Substrates as Revealed by Neutron Reflectometry. *Macromolecules* **1998,** 31, (25), 8893-8906.

45. Ladam, G.; Schaad, P.; Voegel, J. C.; Schaaf, P.; Decher, G.; Cuisinier, F., In Situ Determination of the Structural Properties of Initially Deposited Polyelectrolyte Multilayers. *Langmuir* **1999,** 16, (3), 1249-1255.

46. Mendelsohn, J. D.; Barrett, C. J.; Chan, V. V.; Pal, A. J.; Mayes, A. M.; Rubner, M. F., Fabrication of Microporous Thin Films from Polyelectrolyte Multilayers. *Langmuir* **2000,** 16, (11), 5017-5023.

47. Ouyang, L.; Malaisamy, R.; Bruening, M. L., Multilayer Polyelectrolyte Films as Nanofiltration Membranes for Separating Monovalent and Divalent Cations. *Journal of Membrane Science* **2008,** 310, (1-2), 76-84.

48. Dotzauer, D. M.; Dai, J.; Sun, L.; Bruening, M. L., Catalytic Membranes Prepared Using Layer-by-Layer Adsorption of Polyelectrolyte/Metal Nanoparticle Films in Porous Supports. *Nano Letters* **2006,** 6, (10), 2268-2272.

49. Dotzauer, D. M.; Bhattacharjee, S.; Wen, Y.; Bruening, M. L., Nanoparticle-Containing Membranes for the Catalytic Reduction of Nitroaromatic Compounds. *Langmuir* **2009,** 25, (3), 1865-1871.

50. Stanton, B. W.; Harris, J. J.; Miller, M. D.; Bruening, M. L., Ultrathin, Multilayered Polyelectrolyte Films as Nanofiltration Membranes. *Langmuir* **2003,** 19, (17), 7038-7042.

51. Miller, M. D.; Bruening, M. L., Controlling the Nanofiltration Properties of Multilayer Polyelectrolyte Membranes through Variation of Film Composition. *Langmuir* **2004,** 20, (26), 11545-11551.

52. Malaisamy, R.; Bruening, M. L., High-Flux Nanofiltration Membranes Prepared by Adsorption of Multilayer Polyelectrolyte Membranes on Polymeric Supports. *Langmuir* **2005,** 21, (23), 10587-10592.

53. Hong, S. U.; Miller, M. D.; Bruening, M. L., Removal of Dyes, Sugars, and Amino Acids from NaCl Solutions Using Multilayer Polyelectrolyte Nanofiltration Membranes. *Industrial & Engineering Chemistry Research* **2006,** 45, (18), 6284-6288.

54. Hong, S. U.; Malaisamy, R.; Bruening, M. L., Separation of Fluoride from other Monovalent Anions Using Multilayer Polyelectrolyte Nanofiltration Membranes. *Langmuir* **2007,** 23, (4), 1716-1722.

55. Bruening, M. L.; Dotzauer, D. M.; Jain, P.; Ouyang, L.; Baker, G. L., Creation of Functional Membranes Using Polyelectrolyte Multilayers and Polymer Brushes. *Langmuir* **2008,** 24, (15), 7663-7673.

56. Datta, S.; Cecil, C.; Bhattacharyya, D., Functionalized Membranes by Layer-by-Layer Assembly of Polyelectrolytes and in Situ Polymerization of Acrylic Acid for Applications in Enzymatic Catalysis. *Industrial & Engineering Chemistry Research* **2008,** 47, (14), 4586-4597.

57. Dai, J.; Baker, G. L.; Bruening, M. L., Use of Porous Membranes Modified with Polyelectrolyte Multilayers as Substrates for Protein Arrays with Low Nonspecific Adsorption. *Analytical Chemistry* **2005,** 78, (1), 135-140.

Chapter 2

Preparation of Ion-Exchange Membranes through Layer-by-Layer Adsorption

2.1 Introduction

Ion exchange is the mechanism most commonly employed for capture of proteins and viruses in membrane absorbers because these macromolecules are charged bio-particles under certain pH values.[1, 2] The preparation of ion-exchange membranes, as well as other membrane absorbers, typically includes three steps: (1) synthesis of the base porous membrane (either commercially or in the lab); (2) activation of the bare membrane for physical or chemical modification; and (3) introduction of ion-exchange or other affinity groups in the activated membranes via polymerization or small molecule attachment.[3] To maintain a high permeability, the modification process should not greatly alter the micro- or macro-porosity of the membrane. Additionally, the modifications should not result in a surface that is susceptible to non-specific binding, as this would greatly decrease selectivity.

A number of polymerization methods such as in-situ copolymerization,[3, 4] radiation-induced grafting,[5-8] and other surface-initiated polymerization techniques[2, 9-11] have been employed to create ion-exchange membranes. These methods modify the pores of the membrane with polymer films that can potentially provide a large number of binding sites. However, the synthesis of polymer brushes is often complex, and more importantly, the brushes may significantly decrease the membrane permeability. Because of its simplicity and fine control over film thickness, the layer-by-layer (LBL) film-

formation method provides an attractive alternative to polymerization for membrane modification. In this case, LBL adsorption simply involves circulating polyelectrolyte solutions through the porous substrate to allow polyelectrolyte adsorption inside the membrane pores (Figure 2.1). Alternating deposition of polycations and polyanions, with rinsing between adsorption of each layer, leads to the formation of polyelectrolyte multilayers, and cation-exchange and anion-exchange membranes result from terminating the films with polyanion and polycation layers, respectively.

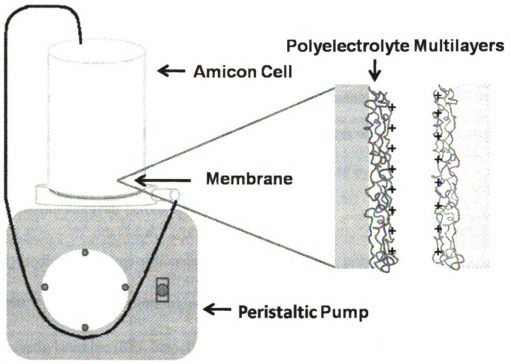

Figure 2.1: Schematic diagram of the apparatus used to modify membranes via LBL adsorption. The enlargement of the membrane shows a single pore modified with a polyelectrolyte multilayer that terminates with a polycation.

This chapter presents the detailed procedure for LBL modification of membranes along with attenuated total reflectance-Fourier transform infrared spectroscopy (ATR-FTIR) and streaming potential measurements that confirm the adsorption of

polyelectrolytes. I also examine how the hydraulic permeability of the membranes varies with the number of adsorbed polyelectrolyte layers.

2.2 Experimental

2.2.1 Materials

Hydrophilic nylon and polyethersulfone (PES) membrane filters (25 mm disks) with 5 μm nominal pore sizes and thicknesses of ~80 and ~135 μm, respectively, were purchased from GE Osmonics. Regenerated cellulose (RC) membranes (Whatman, 47 mm discs) with a thickness of 75 μm and a 1 μm nominal pore size were cut to a diameter of 25 mm before use. Hydrophilic polyvinylidene difluoride (PVDF) membranes (25 mm discs) with a thickness of 125 μm and a nominal pore size of 5 μm were obtained from Millipore. Finally, hydrophilic nylon sheets with a 1.2 μm average pore diameter and a thickness of ~110 μm were kindly provided by Pall Corporation and were cut to 25 mm diameter before use.

Poly(sodium 4-styrene-sulfonate) (PSS, M_w = 70,000), poly(acrylic acid) (PAA, M_w = 70,000, 25% aqueous solution), poly(allylamine hydrochloride) (PAH, M_w = 15,000), polyethylenimine (PEI, branched, M_w = 25,000), and poly(diallyldimethylammonium chloride) (PDADMAC, 20 wt % in water, M_w = 100,000-200,000) were purchased from Aldrich. All solutions were prepared using analytical grade chemicals and deionized water (Milli-Q, 18.2 MΩ·cm).

2.2.2 Membrane Modification

Nylon, PES, RC, and PVDF membranes were modified with polyelectrolytes using LBL deposition. For this procedure, the membrane was placed in an Amicon 8010 membrane cell (Millipore), and a solution containing 0.02 M PSS and 0.5 M NaCl was circulated through the membrane for 15 minutes (flow rate at around 76 cm/h) using a peristaltic pump. After passing 10 mL of H_2O through the membrane, a polycation (PAH, PEI, or PDADMAC) was deposited in the same manner prior to rinsing with 10 mL of H_2O. Subsequent polyanion and polycation layers were deposited similarly. The pH values of PSS, PAA, PAH, PEI, and PDADMAC deposition solutions were adjusted to 4, 4, 4, 9, and 6, respectively, with 0.1 M NaOH or HCl, and all deposition solutions contained 0.02 M polymer and 0.5 M NaCl, unless otherwise noted. (Polymer concentrations are always given with respect to the repeating unit.) Membranes were dried thoroughly with N_2 after deposition and rinsing of the final layer.

2.2.3 ATR-FTIR Spectroscopy

ATR-FTIR spectroscopy (Perkin Elmer Spectrum One) was used to characterize membranes modified with polyelectrolytes. A diamond crystal embedded in a flat metal stage was cleaned gently with soft wipes and kept dry before use. The membrane was pressed against the crystal with a lever arm, and a spectrum of the bare diamond crystal in air was used as a background. All spectra were recorded using 16 scans at 4 cm^{-1} resolution. Membranes must be dried carefully with N_2 before use to ensure the absence of unwanted water peaks.

2.2.4 Streaming Potential Measurements

Streaming potential measurements were conducted using a streaming potential analyzer (BI-EKA, Brookhaven Instruments, Holtsville, NY) with an asymmetric clamping cell (Anton Paar, Graz, Austria).[12, 13] The cell contains a 10 × 20 mm grooved poly(methyl methacrylate) (PMMA) spacer, and the 50 × 50 mm membrane substrate (1.2 μm nylon) was placed against the PMMA spacer and sandwiched by another larger PMMA block. The potential across the cell was measured using Ag/AgCl electrodes while flowing a 1 mM KCl solution through the channels of the PMMA spacer, and the streaming potential of a PMMA sheet was determined prior to measuring the streaming potential of the membrane. The zeta potentials (ζ) of PSS- and PEI-terminated nylon membranes were calculated using the following equation:

$$\varsigma = 2\varsigma_{Avg} - \varsigma_{PMMA}$$

where ζ_{Avg} is the zeta potential determined with the membrane against the PMMA spacer, and ζ_{PMMA} is the potential of the bare PMMA film.[14] (This equation corrects for the fact that when measuring the streaming potential of the membrane, the potential is an average of the membrane and the PMMA spacer.) The final ζ potentials were calculated from an average of the streaming potentials in two flow directions in two different measurements.

2.2.5 Determination of Hydraulic Permeability

Using a pressurized feed tank connected to an Amicon cell, the permeabilities of the membranes to pure water were determined after deposition of each polyelectrolyte layer. The feed tank was filled with deionized water, the system was pressured with N_2

to 0.69 bar, and the permeate was collected over specific time intervals to determine the pure water flux. (The effective membrane area in the cell is 3.1 cm^2.) Three measurements of permeate flux were recorded and averaged after each deposition step. All measurements were done with two membranes to ensure reproducibility.

2.3 Results and Discussion

2.3.1 ATR-FTIR Characterization of Modified Membranes

Successful membrane modification occurred through alternating LBL deposition of the polyelectrolytes shown in Figure 2.2. We generally employ PSS as the initial polyelectrolyte because it adheres well to polymer substrates.[15] Figure 2.3 shows the ATR-FTIR spectra of nylon membranes before and after deposition of PSS-terminated polyelectrolyte films. Although most of the peaks in the spectra stem from the nylon membrane, peaks due to the sulfonate moieties of PSS (1010 cm^{-1} and 1040 cm^{-1}) provide evidence for successful film formation. Because the intensities of peaks in ATR-FTIR spectra vary with the quality of the contact with the ATR crystal, the use of relative rather than absolute absorbances is a better indicator of the adsorption of polyelectrolyte films. Table 2.1 lists the ratios of the sulfonate absorbances to the amide I absorbance (1633 cm^{-1}) of the nylon substrate.

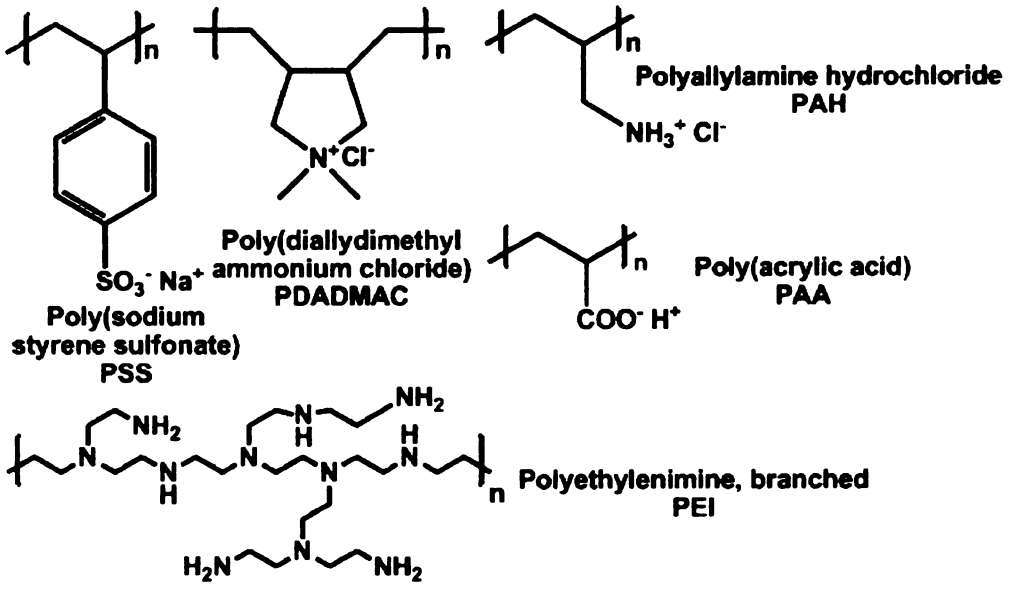

Figure 2.2: Structures of polyelectrolytes used in this study. (The protonation sites for PEI have not been determined.)

These ratios increase with the number of PSS layers in the film, which is consistent with LBL growth. Noticeably, the increase of the ratios from the bare membrane to the first PSS layer is not significant, especially compared to the increases after addition of the second and third layers. Apparently, little PSS adsorbs to the membrane in the first deposition step, presumably because of the negative charge on the membrane surface (see below).

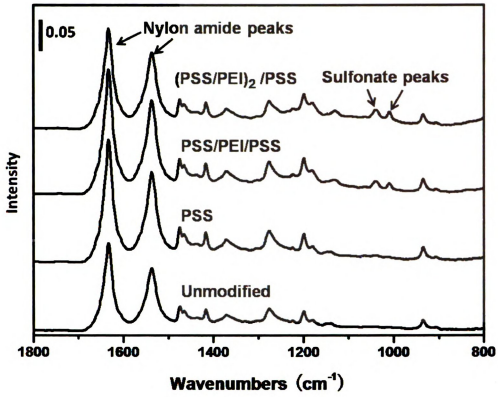

Figure 2.3: ATR-FTIR spectra of 5-μm nylon membranes before and after modification with PSS/PEI films. The ratios of the sulfonate absorbances to the amide I absorbance increase with the deposition of more PEI/PSS layers.

Table 2.1: Ratios of sulfonate absorbances to amide I absorbances for 5-mm nylon membranes modified with PSS/PEI films.

	1010 cm^{-1}:1633 cm^{-1}	**1040 cm^{-1}:1633 cm^{-1}**
Unmodified	0.001	0.002
PSS	0.003	0.005
PSS/PEI/PSS	0.013	0.024
$(PSS/PEI)_2$ /PSS	0.022	0.035

2.3.2 Zeta Potentials of Modified Membranes

Zeta Potentials of polyelectrolyte-modified nylon membranes were determined to further confirm the attachment of polymer films. Due to the specific requirements of the measurement (50 × 50 mm sample size) and the sizes of our membranes, we used 1.2-μm instead of 5-μm nylon membranes for these measurements. Because the substrates are both nylon, the results for the membranes with smaller pores should also be applicable to the membranes with larger pores. Figure 2.4 shows the zeta potential change with the addition of PSS/PEI films. The negative charge on the bare membrane is a common feature of filtration membranes and, as mentioned above, likely contributes to the low PSS adsorption during deposition of the first layer. After the deposition of the initial PSS layer, the zeta potential remained negative as would be expected.

With the further deposition of PEI and PSS layers, zeta potentials alternated between positive and negative values. Interestingly, PEI-capped membranes have higher zeta potential magnitudes than PSS-capped membranes, which potentially suggest that for membranes modified by LBL adsorption of these polyelectrolytes, anion-exchange membranes may have higher binding capacities than cation-exchange membranes.

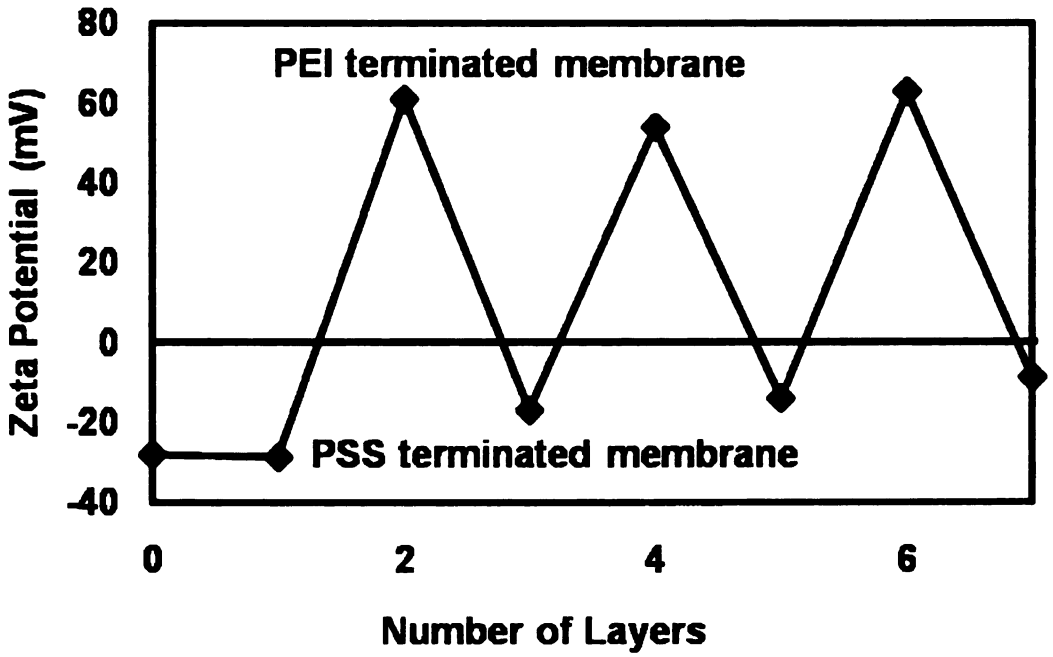

Figure 2.4: Zeta potentials of nylon membranes modified with PSS/PEI films. Films with an odd number of layers terminate with PSS, and films with an even number of layers end in PEI. (These measurements were performed on 1.2-μm nylon membranes rather than 5-μm membranes because the latter were not available with sufficient surface areas for streaming potential measurements.)

2.3.3 Hydraulic Permeabilities of Modified Membranes

One concern in modifying membranes using the LBL method is that the film may plug membrane pores, and the spongy structure of many polymeric membranes may be particularly prone to pore blocking. To avoid plugging, we use membranes with pore sizes > 1 μm. Figure 2.5 shows how the pressure-driven (0.69 bar) pure water flux through 5-μm nylon membranes declines after each step in the deposition of $(PSS/PEI)_3/PSS$, $(PSS/PAH)_3/PSS$ and $(PSS/PDADMAC)_3/PSS$ films. The flow rate through the membrane decreases only slightly after each modification step, and the final

flux through membranes modified with 3.5-bilayer films is still ~80% of that through the bare membrane. The polyelectrolytes apparently occlude only a small fraction of the pore volume.

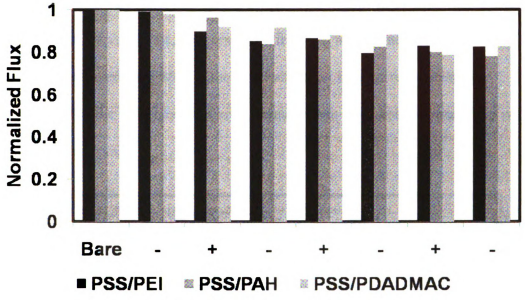

Figure 2.5: Normalized pure water flux through 5-μm nylon membranes before and after modification with PSS/PEI, PSS/PAH, and PSS/PDADMAC films. The "-" and "+" symbols represent deposition of additional polyanion and polycation layers, respectively. The flux was measured at 0.69 bar and normalized to the flux through the bare membrane, which was 2.0±0.3 $cm \cdot s^{-1} \cdot bar^{-1}$.

The hydraulic permeability of nylon membranes modified with 3.5-bilayer films is 1.7±0.2 $cm \cdot s^{-1} \cdot bar^{-1}$, which is about 20% higher than the permeability of commercial Sartobind™ ion-exchange membranes, which have a hydraulic permeability of 1.3 $cm \cdot s^{-1} \cdot bar^{-1}$.[16] Pall Mustang™ ion-exchange membranes have a smaller pore size (0.8 μm)[17] and likely a lower permeability than Sartobind™ membranes. The permeability of ion-

exchange membranes is important because high permeabilities allow the use of thicker membranes to increase capacity without creating an unmanageable pressure drop.

Modification of other types of membranes, i.e., 5-μm PVDF, 1-μm RC, and 1.2-μm nylon, with PSS/PEI films also results in a gradual decline in permeability as more layers are added. Nevertheless, the permeabilities of all membranes modified with 3 polyelectrolyte bilayers are ~80% of the permeabilities of the corresponding bare membranes. Thus the LBL process allows filtration with a minimal pressure drop with a wide range of materials.

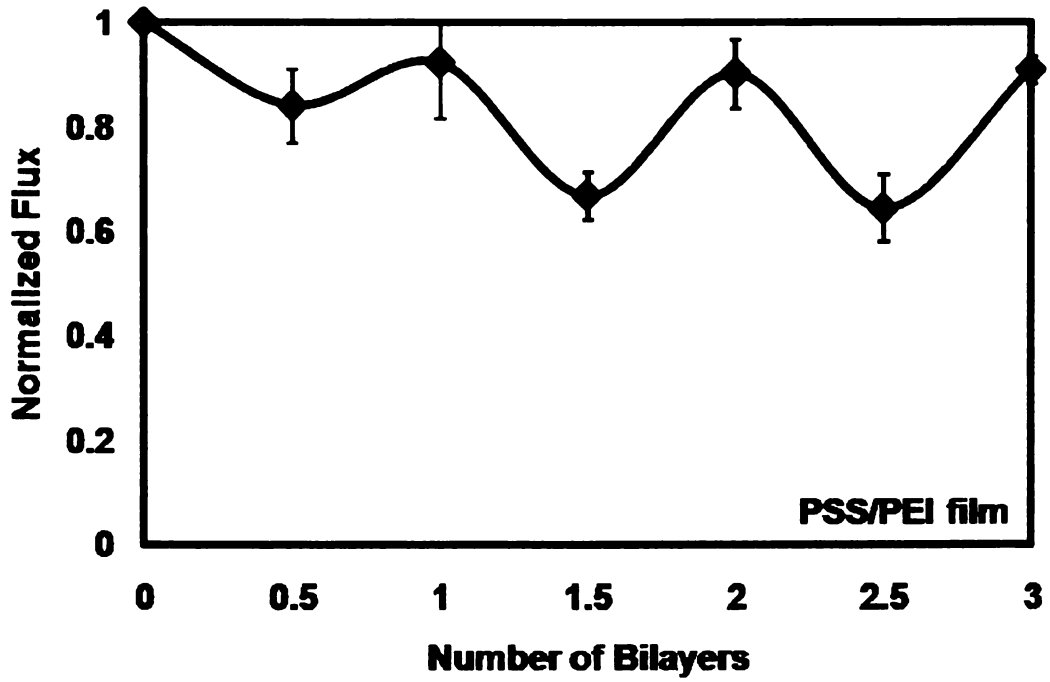

Figure 2.6: Fluxes of pure water through PSS/PEI-modified 5-μm PES membranes under a transmembrane pressure of 0.69 bar. The fluxes are normalized to that through the bare membrane, which was 2.6±0.1 $cm \cdot s^{-1} \cdot bar^{-1}$.

Interestingly, for 5-μm PES membranes, the flux after the deposition of PEI is always higher than that after deposition of the previous PSS layer (Figure 2.6). This

suggests that swelling of PSS-terminated films is greater than that of PEI-terminated films, but only when using PES as a support. Previous studies shows that the support can greatly affect the film structure in the first few layers[18] and that swelling also depends on whether films end in a polycation or a polyanion.[19]

2.4 Conclusions

LBL deposition allows formation of polyelectrolyte multilayers in porous membranes. PSS, PEI, PAH, and PDADMAC can all serve as constituent polyelectrolytes in these films. Increases in the intensities of sulfonate peaks in ATR-FTIR spectra and changes in zeta potentials demonstrate the successful deposition of polyelectrolyte films. The hydraulic permeability of pure water through 5-μm nylon membranes modified with 3.5 bilayers of PSS/PEI is 1.7±0.2 $cm \cdot s^{-1} \cdot bar^{-1}$, which is ~80% of the permeability of a bare membrane and higher than the permeabilities of commercial ion-exchange membranes.

2.5 References

1. Rachel, S.; Binbing, H.; Wickramasinghe, S. R.; Jonathan, O. C.; Peter, C.; Anne, W.; Oscar-Werner, R., Densonucleosis Virus Purification by Ion Exchange Membranes. *Biotechnology and Bioengineering* **2004,** 88, (4), 465-473.

2. Bhut, B. V.; Wickramasinghe, S. R.; Husson, S. M., Preparation of High-Capacity, Weak Anion-Exchange Membranes for Protein Separations Using Surface-Initiated Atom Transfer Radical Polymerization. *Journal of Membrane Science* **2008,** 325, (1), 176-183.

3. Zeng, X.; Eli, R., Membrane Chromatography: Preparation and Applications to Protein Separation. *Biotechnology Progress* **1999,** 15, (6), 1003-1019.

4. Ulbricht, M., Advanced Functional Polymer Membranes. *Polymer* **2006,** 47, (7), 2217-2262.

5. Kawai, T.; Saito, K.; Lee, W., Protein Binding to Polymer Brush, Based on Ion-Exchange, Hydrophobic, and Affinity Interactions. *Journal of Chromatography B* **2003,** 790, (1-2), 131-142.

6. Mika, A. M.; Childs, R. F.; Dickson, J. M.; McCarry, B. E.; Gagnon, D. R., Porous, Polyelectrolyte-Filled Membranes: Effect of Cross-Linking on Flux and Separation. *Journal of Membrane Science* **1997,** 135, (1), 81-92.

7. Ulbricht, M.; Yang, H., Porous Polypropylene Membranes with Different Carboxyl Polymer Brush Layers for Reversible Protein Binding via Surface-Initiated Graft Copolymerization. *Chemistry of Materials* **2005,** 17, (10), 2622-2631.

8. Singh, N.; Husson, S. M.; Zdyrko, B.; Luzinov, I., Surface Modification of Microporous PVDF Membranes by ATRP. *Journal of Membrane Science* **2005,** 262, (1-2), 81-90.

9. Singh, N.; Wang, J.; Ulbricht, M.; Wickramasinghe, S. R.; Husson, S. M., Surface-Initiated Atom Transfer Radical Polymerization: A New Method for Preparation of Polymeric Membrane Adsorbers. *Journal of Membrane Science* **2008,** 309, (1-2), 64-72.

10. Bhut, B. V.; Husson, S. M., Dramatic Performance Improvement of Weak Anion-Exchange Membranes for Chromatographic Bioseparations. *Journal of Membrane Science* **2009,** 337, (1-2), 215-223.

11. Sun, L.; Dai, J.; Baker, G. L.; Bruening, M. L., High-Capacity, Protein-Binding Membranes Based on Polymer Brushes Grown in Porous Substrates. *Chemistry of Materials* **2006,** 18, (17), 4033-4039.

12. Adusumilli, M.; Bruening, M. L., Variation of Ion-Exchange Capacity, ζ Potential, and Ion-Transport Selectivities with the Number of Layers in a Multilayer Polyelectrolyte Film. *Langmuir* **2009,** 25, (13), 7478-7485.

13. Ouyang, L.; Malaisamy, R.; Bruening, M. L., Multilayer Polyelectrolyte Films as Nanofiltration Membranes for Separating Monovalent and Divalent Cations. *Journal of Membrane Science* **2008,** 310, (1-2), 76-84.

14. Walker, S. L.; Bhattacharjee, S.; Hoek, E. M. V.; Elimelech, M., A Novel Asymmetric Clamping Cell for Measuring Streaming Potential of Flat Surfaces. *Langmuir* **2002,** 18, (6), 2193-2198.

15. Dotzauer, D. M.; Dai, J.; Sun, L.; Bruening, M. L., Catalytic Membranes Prepared Using Layer-by-Layer Adsorption of Polyelectrolyte/Metal Nanoparticle Films in Porous Supports. *Nano Letters* **2006,** 6, (10), 2268-2272.

16. http://www.sartorius.hr/pdf/bio/kromatografija/ionski_izmjenjivaci.pdf.

17. http://labfilters.pall.com/catalog/laboratory_19993.asp.

18. Kolasinska, M.; Warszynski, P., The Effect of Support Material and Conditioning on Wettability of PAH/PSS Multilayer Films. *Bioelectrochemistry* **2005,** 66, (1-2), 65-70.

19. Miller, M. D.; Bruening, M. L., Correlation of the Swelling and Permeability of Polyelectrolyte Multilayer Films. *Chemistry of Materials* **2005,** 17, (21), 5375-5381.

Chapter 3

Binding of Au Nanoparticles and Lysozyme to Ion-Exchange Membranes

3.1 Introduction

Separation of proteins and other biomolecules with ion-exchange membranes is attractive because of the low pressure drop and rapid mass transport available in membrane-based separations.[1-3] Primary performance metrics for characterization of separations with ion-exchange membranes include permeability, dynamic binding capacity, selectivity, and recovery. Low permeabilities limit the flux through the membrane, whereas binding capacity, selectivity and recovery are measures of the separation effectiveness.

This chapter examines the binding capacities of ion-exchange membranes prepared by layer-by-layer (LBL) deposition of polyelectrolytes. Citrate-stabilized Au nanoparticles serve as model negatively charged analytes, and Au nanoparticle immobilization on polyelectrolytes was previously applied for development of catalytic membranes.[4] Importantly, the Au nanoparticles we synthesized have a diameter of 12±1 μm, This diameter is similar to that of some viruses, which are also typically negatively charged, so studies of Au nanoparticle binding should be relevant to virus capture. Lysozyme,a well-known model protein that is highly positively charged, provides a convenient substrate for examining the binding performance of cation-exchange membranes. This work investigates the binding capacities of a series of membranes prepared by deposition of a variety of polyelectrolytes in several different porous

substrates. The high permeabilities of these membranes allow the use of membrane stacks to increase capacity.

3.2 Experimental

3.2.1 Materials

All membranes and polyelectrolytes were introduced in Chapter 2. Gold (III) chloride trihydrate (≥ 99.9 trace metal basis), sodium citrate, and lysozyme (from chicken egg white) were purchased from Aldrich. All buffers were prepared using analytical grade chemicals and deionized water (Milli-Q, 18.2 MΩ·cm).

3.2.2 Scanning Electron Microscopy

Membrane samples were characterized by scanning electron microscopy (SEM) using a Hitachi S-4700 II field-emission scanning electron microscope. Prior to imaging, samples were fractured with tweezers in liquid nitrogen, and the cross section was coated with 10 nm of Au using a Pelco SC-7 sputter coater. The cross-sectional images were used to determine the thicknesses of 5-μm nylon and PES membranes (Figure 3.1), and images of cross sections and the top and rear of membranes were taken to examine adsorption of Au nanoparticles.

3.2.3 Binding of Au Colloids to Modified Membranes

With the polyelectrolyte-modified membrane in the Amicon cell (exposed membrane area of 3.1 cm^2), a 0.05 mM Au-colloid solution (concentration is defined as the molarity of Au atoms) was passed through the membrane using a peristaltic pump.[4] The flow rate was adjusted by varying the spinning rate of the pump and determined by

measuring the permeate volume over a period of time. To determine the concentration of Au colloids in the feed or permeate, the absorbance of the solution at 519 nm (λ_{max}) was converted to concentration with the linear calibration curve shown in Figure 3.2a.

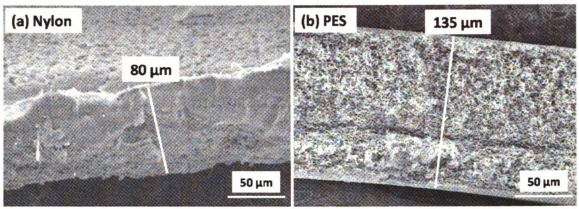

Figure 3.1: Cross-sectional SEM images of 5-µm (a) nylon and (b) PES membranes. The measured thicknesses are 80 and 135 µm for nylon and PES, respectively. Both images were taken at 15,000 × magnification.

3.2.4 Binding of Lysozyme to Modified Membranes or Membrane Stacks

With one or more polyelectrolyte-modified membranes placed in an Amicon cell, a solution containing 0.1 mg/mL lysozyme in 20 mM phosphate buffer (pH 7.2) was forced through the modified membrane or membrane stack at a constant flux using a peristaltic pump. Permeate was collected in small test tubes, and the volume in each tube was determined gravimetrically, assuming the density of the permeate to be 1 mg/mL. Thirty-µL aliquots of each permeate sample were mixed with 1.5 mL Coomassie protein assay reagent (1:50 v/v), and the absorbance of this solution at 585 nm was obtained relative to phosphate buffer mixed with Coomassie reagent. Absorbances were determined using a Perkin-Elmer Lambda 4 UV-Vis spectrophotometer, and the

concentration of lysozyme in the permeate was determined using a calibration curve (Figure 3.2b).

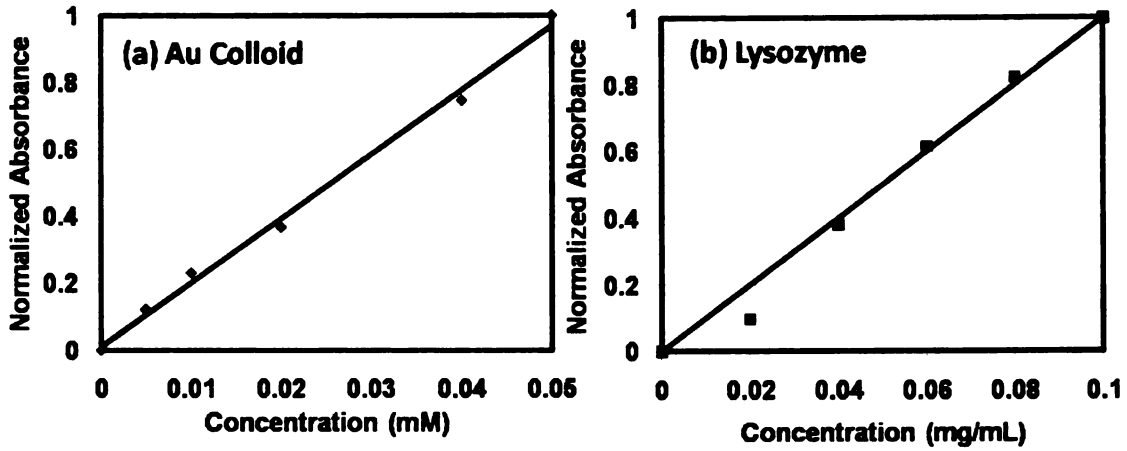

Figure 3.2: Calibration curves for (a) Au colloids and (b) lysozyme. Absorbances are normalized to the absorbances of the feed solutions, 0.05 mM Au or 1.0 mg/mL lysozyme. In (b), the solutions were mixed with Coomassie reagent (see text).

3.2.5 Calibration for Analysis of Au-Colloid and Lysozyme Solutions

For Au colloids, a series of solutions containing 0.05 mM, 0.04 mM, 0.02 mM, 0.01 mM, 0.005 mM and 0 mM Au (concentrations refer to the total moles of gold atoms) were prepared in deionized water, and the absorbances at 519 nm were measured with a UV-Vis spectrophotometer. Pure deionized water was used as background. The calibration curve in Figure 3.2a shows a linear correlation between the absorbance and concentration with an R^2 value of 0.995. For lysozyme, a series of solutions containing 0.1, 0.08, 0.06, 0.04, 0.02, 0.01 and 0 mg/mL lysozyme were prepared in phosphate buffer (pH 7.2) and mixed with Coomassie reagent as described above. The calibration curve in Figure 3.3b shows a linear relationship between absorbance and concentration with a correlation coefficient of 0.986.

3.3 Results and Discussion

3.3.1 Polycation-Terminated Films for Binding of Au Colloids

The deposition of polycation-terminated films in membranes should create anion-exchange materials because of the positively charged film surface. Similarly, films terminated with a polyanion should function as cation exchangers. In investigations of anion exchange, we examined breakthrough curves for binding of citrate-stabilized Au colloids to polycation-terminated films in membranes. The Au colloids have a strong optical absorbance that facilitates their analysis, and previous studies show that binding of gold colloids to polyelectrolyte-coated membranes yields catalytic reactors.[4-6]

Figure 3.3 shows the breakthrough curves for passage of Au-colloid suspensions through 5-μm nylon membranes coated with 1-bilayer PSS/PEI, PSS/PAH, and PSS/PDADMAC films. The PEI-containing film binds the most Au, and breakthrough is less than 10% for about 36 mL of suspension, or over 1400 membrane volumes. The binding capacity of the PEI-terminated films is 27 mg/mL at 80% breakthrough (defined as the capacity when the permeate concentration is 80% of the feed value) and 14 mg/mL for 10% breakthrough. The PAH and PDADMAC films give binding capacities of 8 and 12 mg/mL, respectively, for 80% breakthrough. The branched structure of the PEI may lead to a higher density of ion-exchange sites and a higher binding capacity.

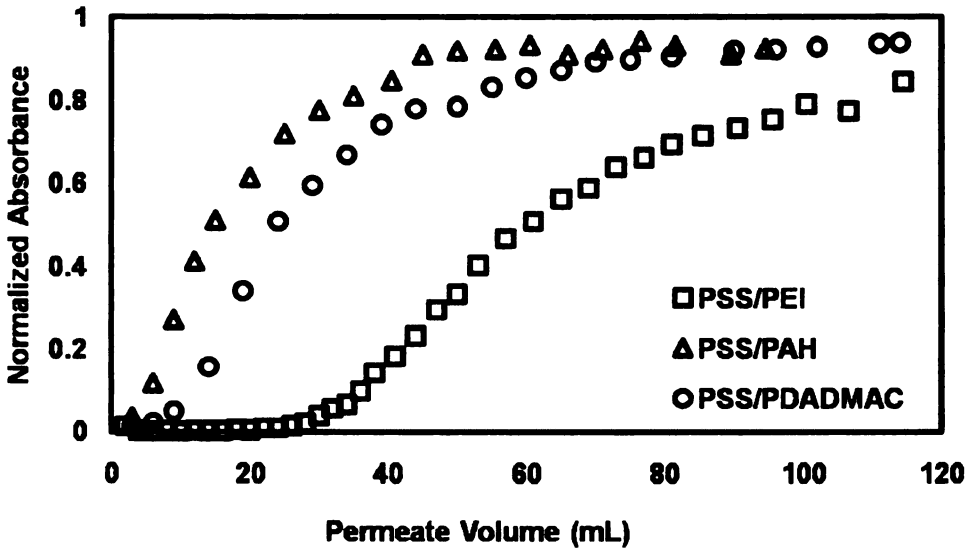

Figure 3.3: Breakthrough curves for passage of Au-colloid solutions through 5-μm nylon membranes modified with 1-bilayer PSS/PEI, PSS/PAH, and PSS/PDADMAC films. Absorbance, which is normalized to the absorbance of the feed solution, is proportional to colloid concentration. The colloid feed solution contained 0.05 mM Au and was pumped through the membranes at a flux of 19 cm/h. Curves are representative of experiments with at least two membranes.

We also examined Au colloid breakthrough curves for membranes modified with 2- and 3- bilayer films. Figure 3.4 shows a gradual increase in Au-colloid binding with the addition of more PSS/PEI layers. Adsorption of a second PSS/PEI bilayer increases binding capacities by about 15 %, whereas deposition of a third PSS/PEI bilayer improves capacity by an additional 20%. Deposition of more polyelectrolyte layers likely yields a more continuous film with increased surface charge and more ion-exchange sites. Nevertheless, although the 1-bilayer film has fewer ion-exchange sites than 2- and 3-bilayer films, the zeta potentials of PEI-terminated membranes do not vary significantly with the number of PSS/PEI bilayers (see Figure 2.4). The majority of the anion-exchange sites may be inside the plane of shear that defines the zeta potential.

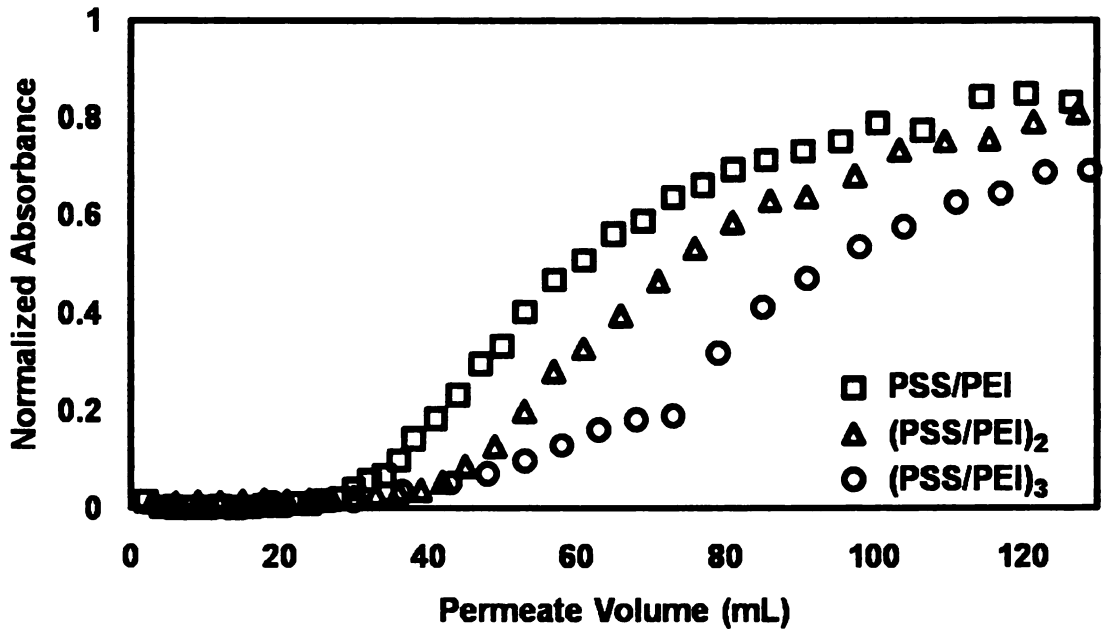

Figure 3.4: Breakthrough curves for passage of Au-colloid solutions through 5-μm nylon membranes modified with 1, 2, and 3 bilayers of PSS/PEI. The feed solution contained 0.05 mM Au and was pumped through the membrane at a flux of 19 cm/h. Curves are representative of experiments with at least two membranes.

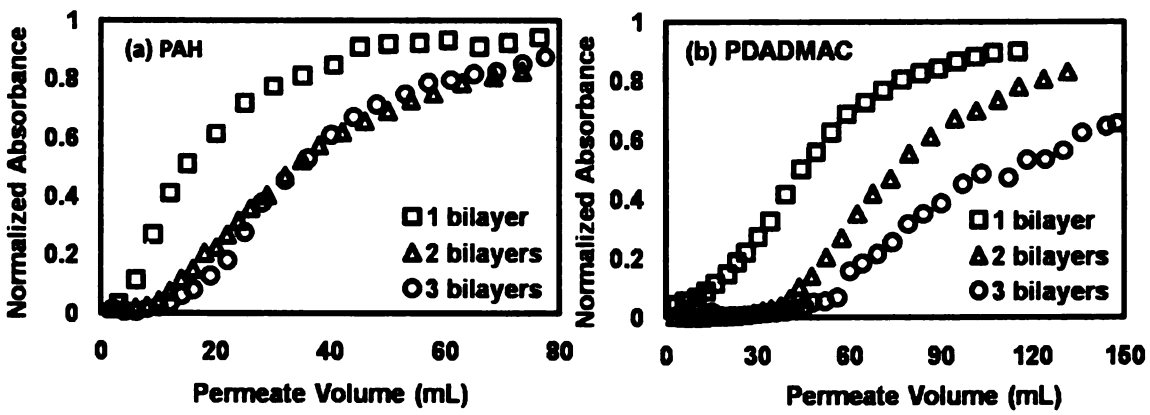

Figure 3.5: Breakthrough curves for the passage of Au-colloid solutions (0.05 mM Au) through 5-μm nylon membranes modified with 1, 2, and 3 bilayers of (a) PSS/PAH and (b) PSS/PDADMAC. The permeate absorbance is normalized to the absorbance in the feed, and the solution was passed through the membrane at a flux of 19 cm/h.

Nylon membranes modified with 1, 2, and 3 bilayers of PSS/PAH and PSS/PDADMAC also show increases in binding capacity upon with the addition of more bilayers (Figure 3.5).

Table 3.1 summarizes the binding capacities of polyelectrolyte films with different numbers of bilayers. We see gradual increases in binding capacities for all three types of films on going from 1- to 3-bilayers. Interestingly, membranes coated with 3-bilayer PSS/PDADMAC films have the largest binding capacity, but the permeability of these membranes dramatically declines during binding of Au colloids, presumably because of pore clogging. (The peristaltic pump cannot maintain a 19 cm/h flux with these membranes, even with an increase in rotation rate.) The clogging may result from aggregated Au nanoparticles that plug pores. SEM images show a uniform dispersion of Au nanoparticles on $(PSS/PEI)_3$-coated membranes (Figure 3.6a) and significant aggregation of Au nanoparticles on $(PSS/PDADMAC)_3$-coated membranes (Figure 3.6b). The high swelling of PSS/PDADMAC films and a high concentration of cationic sites in the interior of the films may allow the adsorption and aggregation of the Au nanoparticles.

Table 3.1. Au-colloid binding capacities of 5-μm nylon membranes modified with multilayer polyelectrolyte films. The Au-colloid feed solution contained 0.05 mM Au and was passed through the membrane at a flux of 19 cm/h.

Polyelectrolyte Film	[a]Binding Capacity at 80% Breakthrough (mg/mL)		
	1 bilayer	2 bilayers	3 bilayers
PSS/PEI	27	31	37
PSS/PAH	8	19	20
PSS/PDADMAC	12	34	39[b]

[a] Binding capacities are the average of measurements on at least two membranes. The individual values differed from the average by less than 40% and usually by less than 15%.

[b] For these membranes, the capacity is determined at <80% breakthrough in two of three cases because these particular systems sometimes plug. Flux through this particular membrane decreased during the experiment.

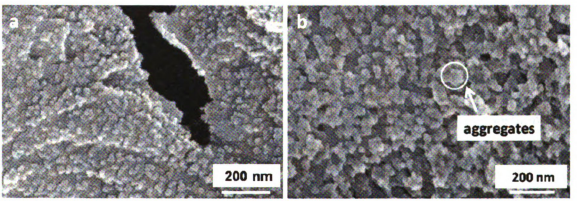

Figure 3.6: SEM images of Au nanoparticles adsorbed on 5-μm nylon membranes modified with 3 bilayers of (a) PSS/PEI and (b) PSS/PDADMAC. Both images were taken at 100,000 × magnification. The circle in the right image shows the aggregates formed on PDADMAC-terminated films.

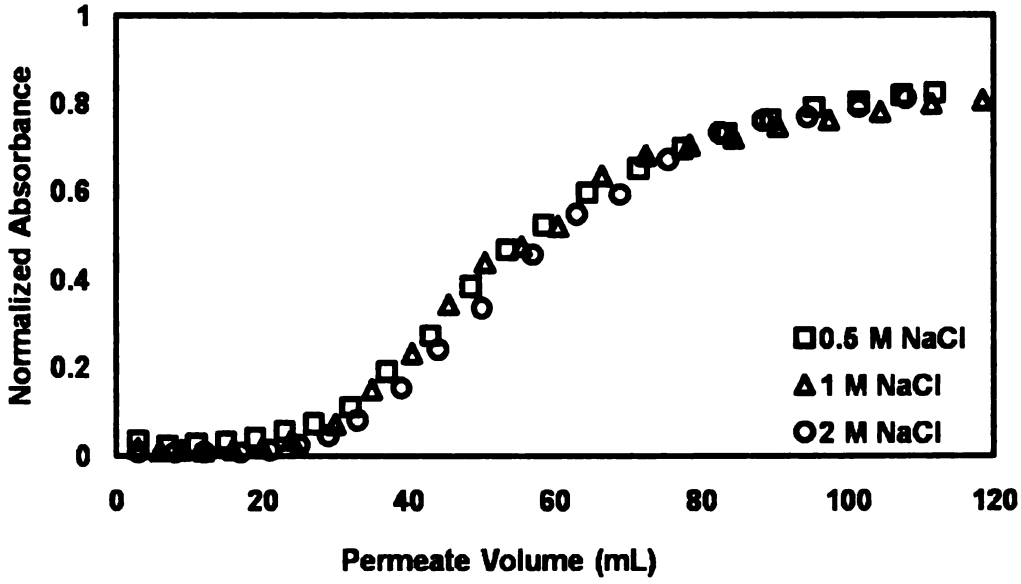

Figure 3.7: Breakthrough curves for the passage of a Au-nanoparticle solution through 5-μm nylon membranes modified with 3 bilayers of PSS/PEI. Solutions employed for the deposition of the last PEI layer contained 0.5 M, 1 M, or 2 M NaCl. The 0.05 mM Au-colloid solution was passed through the membranes at 19 cm/h.

The presence of supporting electrolyte during the deposition of multilayer polyelectrolyte films significantly alters the structures of these films because the salt screens charge on the polyelectrolytes to create more loops and tails in the film.[7] Typically, higher ionic strengths during film deposition give rise to a higher surface charge,[8] which might increase binding capacity. To examine the effect of deposition ionic strength on the binding of Au colloids, we modified several 5-μm nylon membranes with 3 PSS/PEI bilayers and varied the NaCl concentrations in the solutions used to deposit the last layer of PEI. Breakthrough curves for Au-colloid binding are essentially independent of the salt concentration (0.5 to 2 M) used in the deposition of the outer PEI layer (Figure 3.7). Thus, at least for this polyelectrolyte system, deposition of the

terminal layer from a solution of high ionic strength does not increase the number of binding sites for gold colloids.

To briefly examine binding as a function of flux, the Au colloid suspension was passed through modified membrane at fluxes of 19 cm/h and 76 cm/h. As Figure 3.8 shows, the higher flux gives rise to an earlier breakthrough in 5-μm nylon membranes modified with $(PSS/PEI)_3$ films. Similar trends occur with membranes coated with 1 and 2 bilayers of PSS/PEI (Figure 3.9). Thus, the binding in these systems is not simply limited by mass flow into the membrane. However, modeling of colloid binding in this complicated membrane internal structure is beyond the scope of this work.

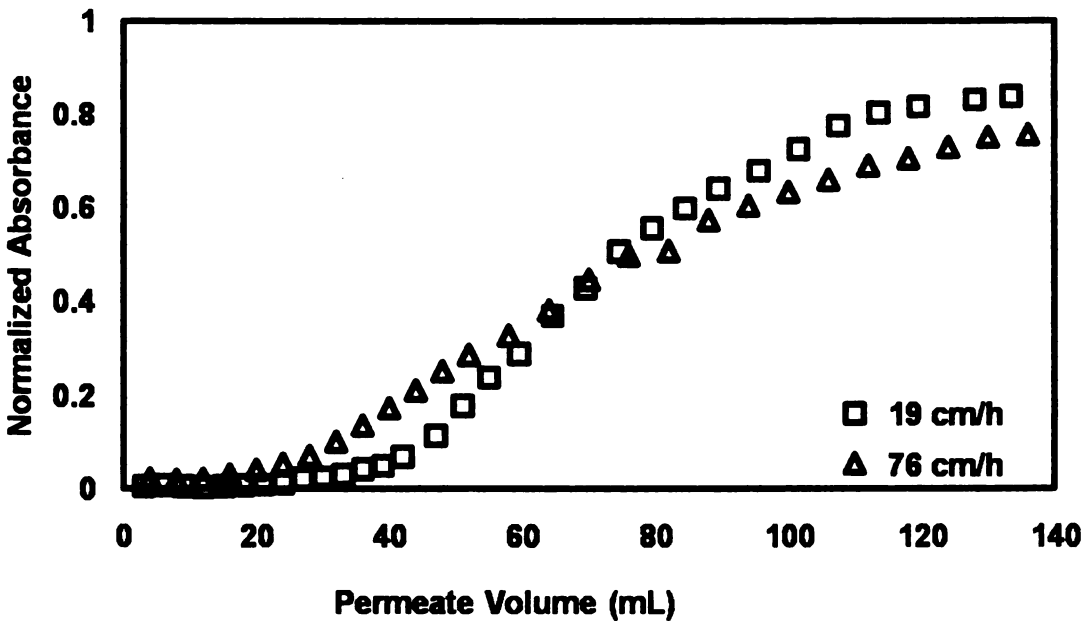

Figure 3.8: Breakthrough curves for passage of a Au-colloid solution through 5-μm nylon membranes modified with $(PSS/PEI)_3$ films. The solution, which contained 0.05 mM Au, was passed through the membranes at fluxes of 19 cm/h and 76 cm/h.

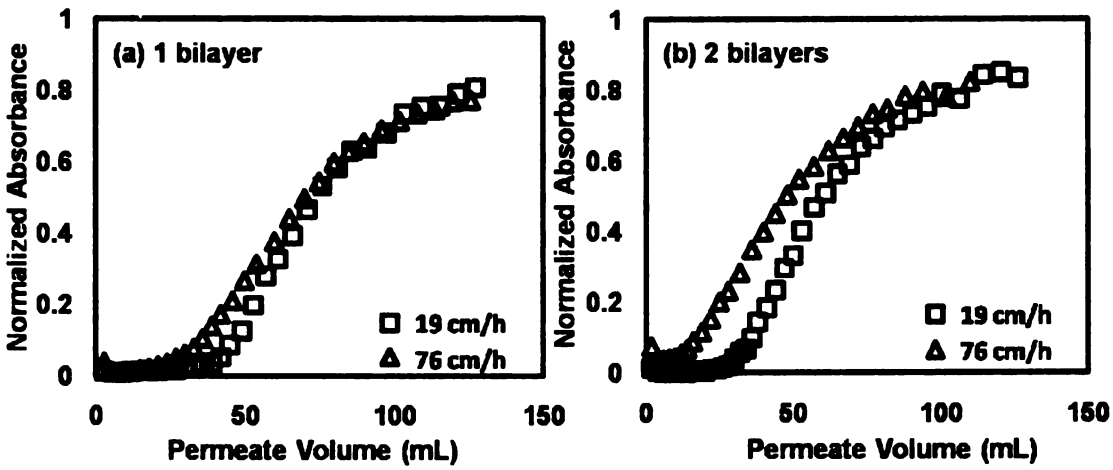

Figure 3.9: Breakthrough curves for the passage of a Au-nanoparticle solution (0.05 mM Au) through 5-μm nylon membranes modified with (a) 2 and (b) 3 bilayers of PSS/PEI. The curves were obtained at fluxes of 19 cm/h and 76 cm/h, and the absorbance is normalized to that in the feed.

Even for the same polyelectrolyte film, both the composition and internal surface area of the substrate membrane should influence binding capacity. The membrane chemistry may affect the structure and the amount of polyelectrolyte deposited, whereas increased surface areas should lead to enhanced binding. Table 3.2 presents Au-nanoparticle binding capacities for $(PSS/PEI)_3$ films in 5-μm nylon, 5-μm PES, 5-μm PVDF, and 1-μm regenerated cellulose membranes. The 5-μm nylon membrane shows the highest binding capacities, especially considering the membrane thicknesses. Although the modified 5-μm PES and nylon membrane have similar binding capacities, the nylon membrane is considerably thinner. The membrane thicknesses determined from SEM cross-sectional images are ~135 μm for PES and ~80 μm for nylon. In the case of the PVDF and RC, the chemical structures of the membranes may resist polyelectrolyte adsorption to give thinner or less uniform films that bind fewer gold

particles. These membranes may also present a lower surface area for polyelectrolyte adsorption. SEM images of the different membranes (Figure 3.10) suggest that the PVDF and RC membranes are much more porous than the nylon and PES substrates.

Table 3.2. Au-colloid binding capacities of 5-μm nylon, PES, and PVDF and 1 μm RC membranes modified with $(PSS/PEI)_3$ films. The binding occurred at a flux of 19 cm/h from a colloid solution containing 0.05 mM Au atoms.

Breakthrough	**Breakthrough Binding Capacity (mg/mL)**			
Level	**Nylon**	**PES**	**PVDF**	**RC**
80%	37±6	29±4	5±4	8±2
10%	20±3	22±5	≤1	≤2

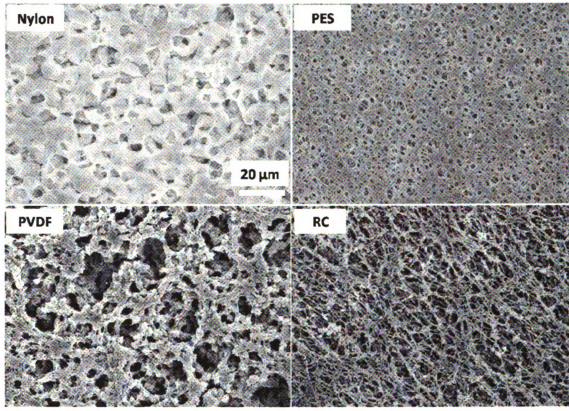

Figure 3.10: SEM images of unmodified nylon, PES, PVDF, and RC membranes at 1,000 × magnification. The scale bar is common for all images.

3.3.2 Cation-Exchange Membranes for Lysozyme Binding

Deposition of polyanion-terminated films in membrane pores should create cation-exchange sites that bind positively charged proteins. Lysozyme has an isoelectric point of 10.7, and in a 20 mM phosphate buffer at pH 7.2, this protein is highly positively charged (~+8) and should bind strongly to polyanions via ionic interactions. In initial experiments, we compared the lysozyme binding capacities of membranes terminated with PSS and PAA. Membranes modified with PSS/PEI/PSS and PSS/PEI/PAA films show distinct binding profiles (Figure 3.11). For the PSS-terminated membrane, breakthrough occurs quickly, partly because of the high lysozyme concentration. PAA-capped films show a more gradual saturation, and the binding capacity of PSS/PEI/PAA-

modified membranes at 80% breakthrough is 14 mg/mL, whereas that for PSS/PEI/PSS films is 11 mg/mL.

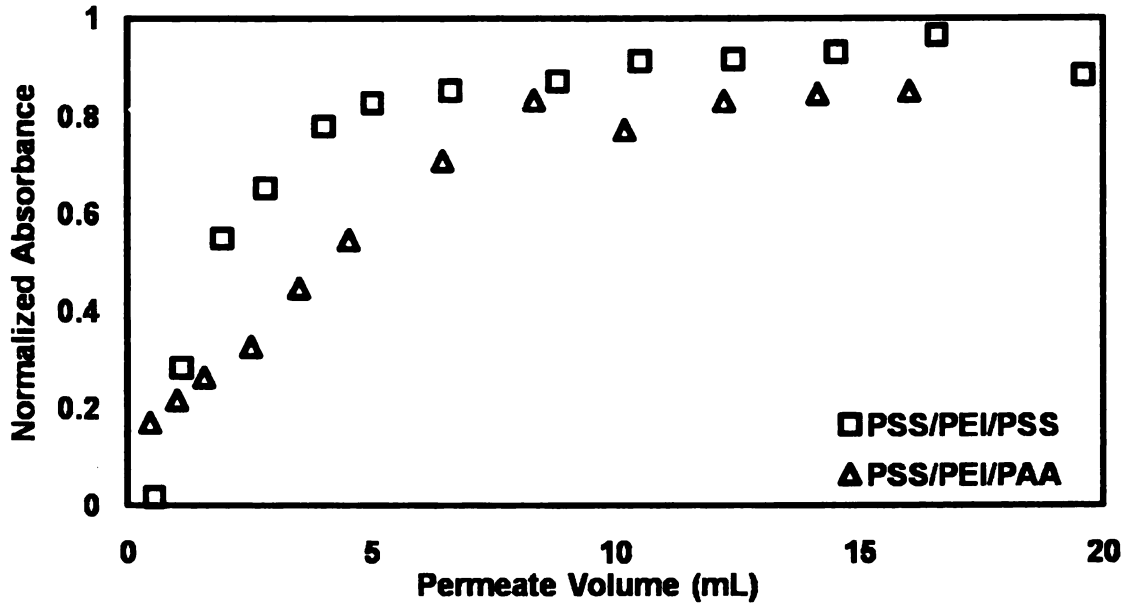

Figure 3.11: Breakthrough curves for the passage of 0.1 mg/mL lysozyme (pH 7.2) through 5-μm nylon membranes modified with PSS/PEI/PSS and PSS/PEI/PAA films. The lysozyme solution was passed through the membranes at a flux of 19 cm/h, and the absorbance of the permeate (after mixing with Coomassie reagent) is normalized to that in the feed.

The charge density of the polycation in the film might also affect the surface charge of polyanion-terminated films and, hence, the binding capacity of membranes modified with such films. However, the lysozyme breakthrough curves for $(PSS/PEI)_3/PSS$, $(PSS/PAH)_3/PSS$, and $(PSS/PDADMAC)_3/PSS$ films in nylon membranes are all similar (Figure 3.12). Thus, the polycation has little effect on binding to these polyanion-terminated films.

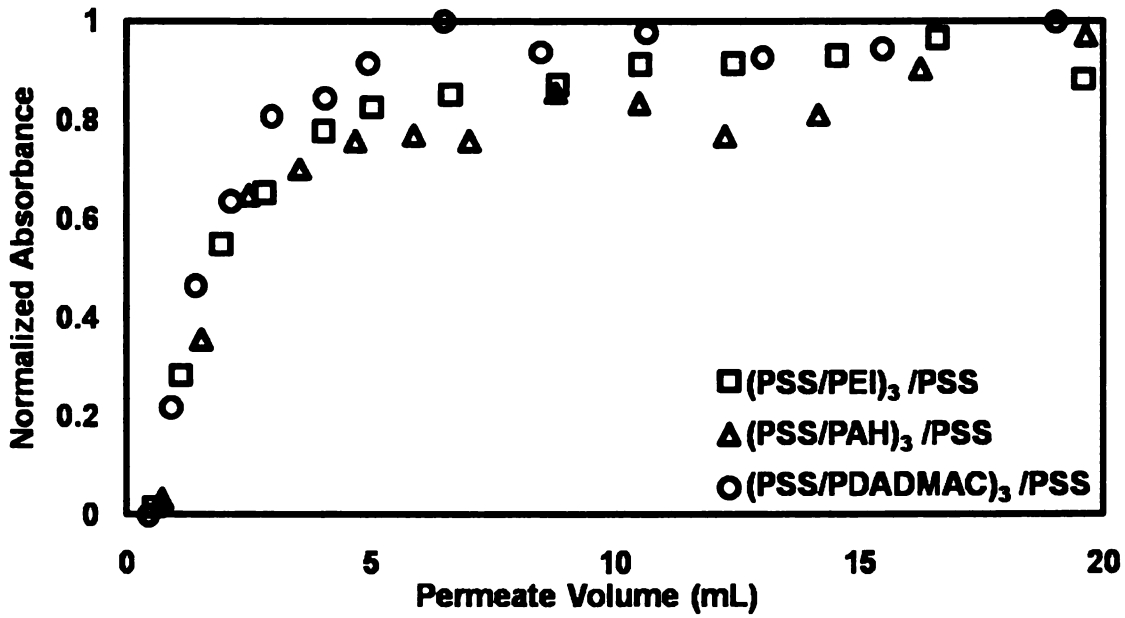

Figure 3.12: Breakthrough curves for the passage of 0.1 mg/mL lysozyme (pH 7.2) through 5-μm nylon membranes modified with 3.5 bilayers of PSS/PEI, PSS/PAH, and PSS/PDADMAC. The lysozyme solution was passed through the membranes at 19 cm/h, and the absorbance (after mixing with Coomassie reagent) is normalized to that in the feed.

In contrast, Figure 3.13 shows that the ionic strength of the solution used to deposit the terminating PSS layer significantly affects lysozyme binding. PSS-terminated membranes prepared using 2 M NaCl in the last PSS deposition solution exhibit capacities that are about twice those for films deposited from solutions containing only 0.5 M NaCl. The salt concentration evidently affects the number of ion-exchanges sites more when depositing PSS than PEI, as binding of gold colloids to PEI-terminated films shows little dependence on the ionic strength of the deposition solution for the last layer (see Figure 3.7).

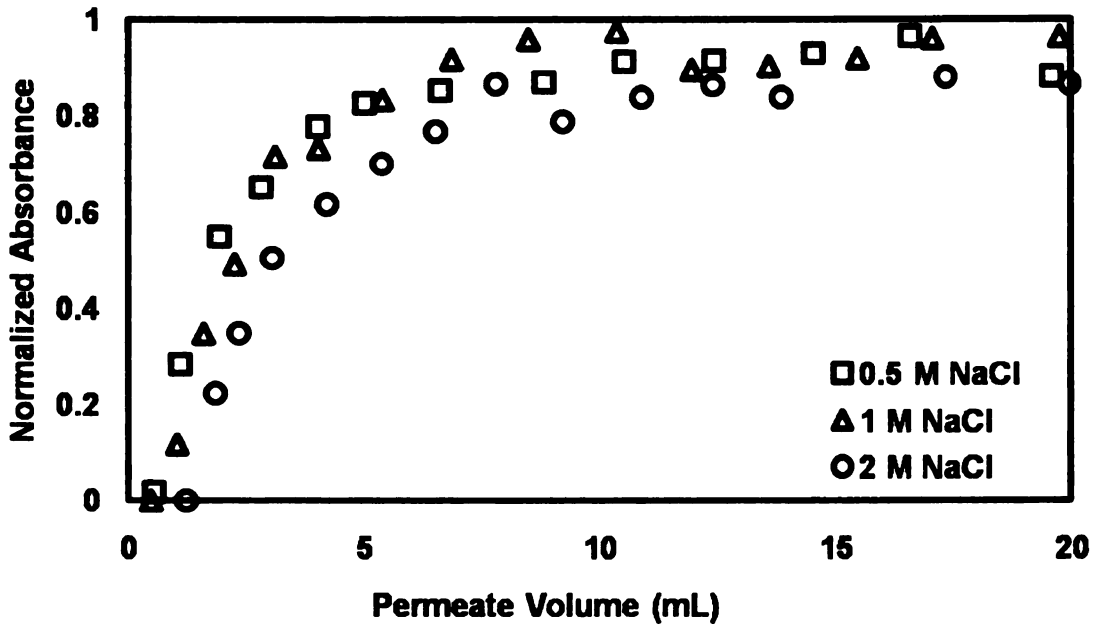

Figure 3.13: Breakthrough curves for binding of 0.1 mg/mL lysozyme (pH 7.2) to 5-μm nylon membranes modified with 3.5 PSS/PEI bilayers. The solutions employed for deposition of the last layer of PSS contained 0.5 M, 1 M, or 2 M NaCl, and the lysozyme solution was passed through the membrane at 19 cm/h.

As with binding of Au colloids to PSS/PEI films, lysozyme binding increases modestly upon going from (PSS/PEI)/PSS films to $(PSS/PEI)_2$/PSS and $(PSS/PEI)_3$/PSS films in membranes (Figure 3.14). The binding capacities at 80% breakthrough are 11, 13, and 16 mg/mL for membranes containing (PSS/PEI)/PSS, $(PSS/PEI)_2$/PSS, and $(PSS/PEI)_3$/PSS films, respectively.

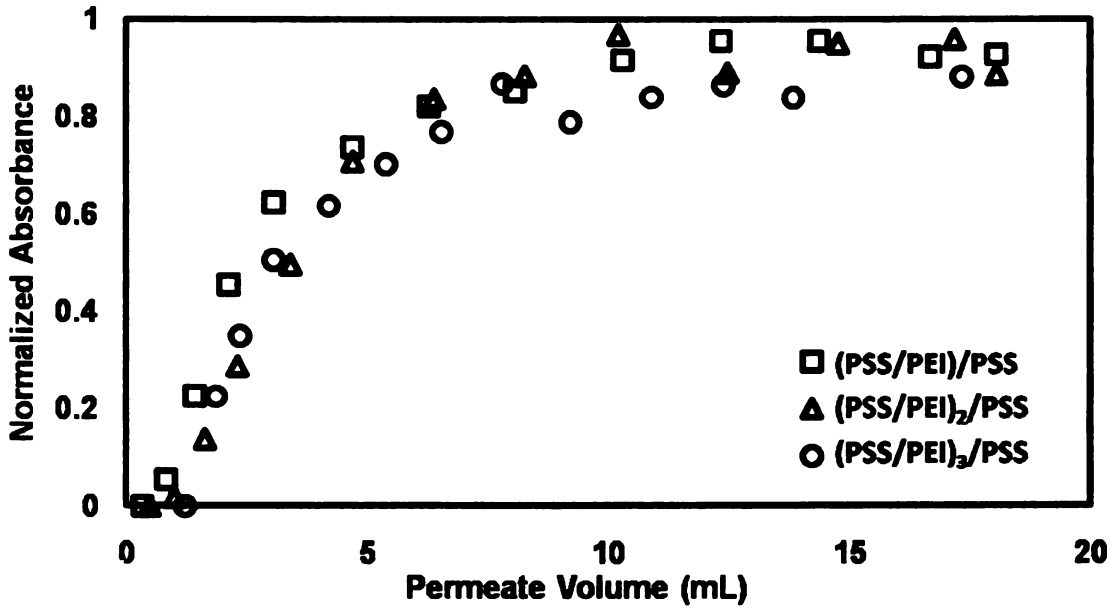

Figure 3.14: Breakthrough curves for binding of 0.1 mg/mL lysozyme (pH 7.2) to 5-μm nylon membranes modified with 1.5, 2.5, and 3.5 bilayers of PSS/PEI. The solution employed for deposition of the last layer of PSS contained 2 M NaCl, and the lysozyme solution was passed through the membrane at 19 cm/h.

After protein binding, we made several attempts to elute the bound lysozyme by passing buffers such as 1 M KSCN in 50 mM phosphate at pH 8 and 2 M NaCl in 50 mM phosphate at pH 10 through the membrane. Unfortunately, these attempts recovered less than 2% of the bound protein. The multiple electrostatic interactions between lysozyme and the polyelectrolyte as well as other non-electrostatic interactions will likely require stronger eluents and longer elution times for recovery of the lysozyme. Thus, these membranes may be most suitable for removing contaminant proteins, viruses, and DNA from solutions, because in those cases elution is not needed for single-use membranes.

3.3.3 Membrane Stacking for Lysozyme Binding

The above results show that the greatest amount of lysozyme binding occurs with 5-μm nylon membranes coated with $(PSS/PEI)_3/PSS$ films prepared with 2 M NaCl present during deposition of the last layer of PSS. However, a single membrane gives a 10% breakthrough capacity of only 6 mg/mL of membrane. Nevertheless, because these membranes are highly permeable, stacking of membranes can increase the capacity while still maintaining low pressure drops.[9] In initial studies, we modified three stacked membranes at once and examined the immobilization of lysozyme in these systems. The 3-membrane stack binds 0.43 mg lysozyme (5.7 mg/mL) at 10% breakthrough, which is essentially 3 times the amount of lysozyme that binds to a single membrane (0.15 mg). Thus, stacking has no deleterious effect on the performance of individual membranes. Figure 3.15 shows breakthrough curves for passage of a lysozyme solution through a stack of 3 membranes at fluxes of 19 and 4 cm/h. The dynamic capacity (10% breakthrough) increases from 5.7 to 7.5 mg/mL on decreasing the flux. Thus, lowering the flux 5-fold improves the binding only to a small extent. Hence, diffusion and kinetic limitations to binding are relatively small.

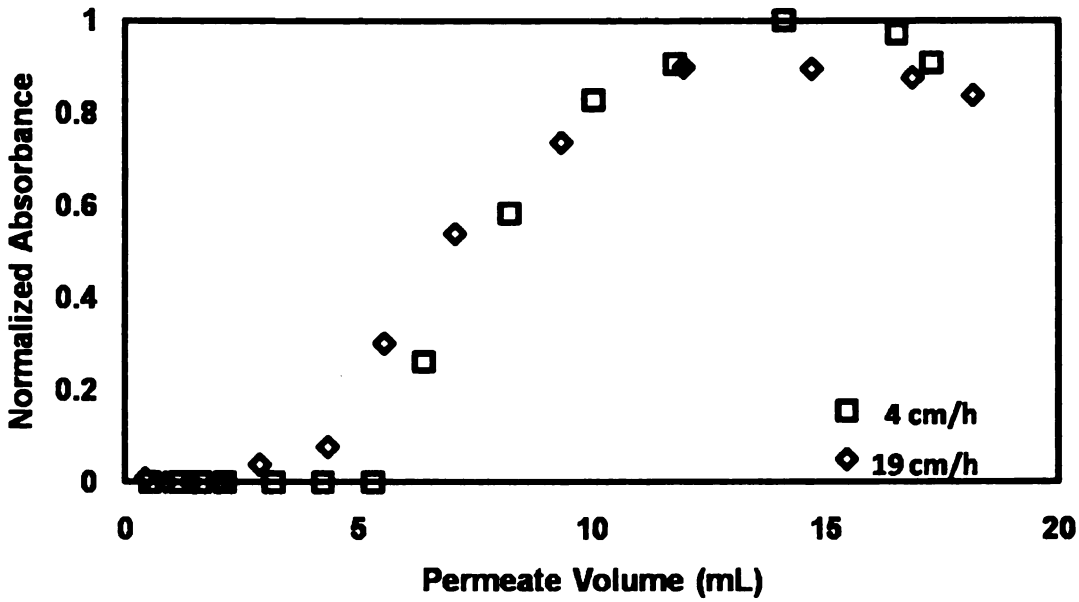

Figure 3.15: Breakthrough curves for binding of lysozyme to membrane stacks. A stack of three 5-μm nylon membranes was modified with 3.5 bilayers of PSS/PEI, and the solution employed for deposition of the last layer of PSS contained 2 M NaCl. The 0.1 mg/mL lysozyme solution was passed through the membrane stacks at 19 and 4 cm/h.

3.4 Conclusions

Membranes modified with polycation-terminated polyelectrolyte films serve as anion-exchange materials that bind negatively charged Au nanoparticles, whereas anion-terminated films bind lysozyme via cation-exchange interactions. When terminated with a polycation, PSS/PAH, PSS/PEI, and PSS/PDADMAC films all bind Au nanoparticles, but PSS/PEI films show the highest capacity without pore blocking. For 5-μm nylon membranes modified with 3 bilayers of PSS/PEI, the Au-colloid binding capacity at 80% breakthrough is 37±6 mg/mL. Increasing the number of polyelectrolyte bilayers from 1 to 3 yields modest (<27%) increases in binding capacity, and nylon and PES membranes showed the most binding, perhaps because of a high internal surface area.

In the case of lysozyme binding, increasing the ionic strength in the deposition solution for the last PSS layer can increase binding capacity by 100%. For the best case, $(PSS/PEI)_3$/PSS-modified nylon membranes exhibit a lysozyme-binding capacity of 16 mg/mL at 80% breakthrough. Moreover, the high permeability of the membranes allows stacking to increase capacity.

3.5 References

1. Knudsen, H. L.; Fahrner, R. L.; Xu, Y.; Norling, L. A.; Blank, G. S., Membrane Ion-Exchange Chromatography for Process-Scale Antibody Purification. *Journal of Chromatography A* **2001,** 907, (1-2), 145-154.

2. Lightfoot, E. N.; Moscariello, J. S., Bioseparations. *Biotechnology and Bioengineering* **2004,** 87, (3), 259-273.

3. Jorg, T.; Mark, E., Alternatives to Chromatographic Separations. *Biotechnology Progress* **2007,** 23, (1), 42-45.

4. Dotzauer, D. M.; Bhattacharjee, S.; Wen, Y.; Bruening, M. L., Nanoparticle-Containing Membranes for the Catalytic Reduction of Nitroaromatic Compounds. *Langmuir* **2009,** 25, (3), 1865-1871.

5. Dotzauer, D. M.; Dai, J.; Sun, L.; Bruening, M. L., Catalytic Membranes Prepared Using Layer-by-Layer Adsorption of Polyelectrolyte/Metal Nanoparticle Films in Porous Supports. *Nano Letters* **2006,** 6, (10), 2268-2272.

6. Bruening, M. L.; Dotzauer, D. M.; Jain, P.; Ouyang, L.; Baker, G. L., Creation of Functional Membranes Using Polyelectrolyte Multilayers and Polymer Brushes. *Langmuir* **2008,** 24, (15), 7663-7673.

7. McAloney, R. A.; Sinyor, M.; Dudnik, V.; Goh, M. C., Atomic Force Microscopy Studies of Salt Effects on Polyelectrolyte Multilayer Film Morphology. *Langmuir* **2001,** 17, (21), 6655-6663.

8. Schlenoff, J. B.; Dubas, S. T., Mechanism of Polyelectrolyte Multilayer Growth: Charge Overcompensation and Distribution. *Macromolecules* **2001,** 34, (3), 592-598.

9. Lin, S.-Y.; Suen, S.-Y., Protein Separation Using Plate-and-Frame Modules with Ion-Exchange Membranes. *Journal of Membrane Science* **2002,** 204, (1-2), 37-51.

Chapter 4

Conclusions and Future Work

4.1 Conclusions

This thesis describes a simple and convenient method for the preparation of ion-exchange membranes. Chapter 2 demonstrates the layer-by-layer (LBL) adsorption procedure for modifying polymeric membrane substrates in a flow-through method. ATR-FTIR spectra and zeta potential measurements confirm the attachment of the polyelectrolyte films to the porous substrates. Hydraulic permeabilities of the membranes decrease by only 20% after addition of 3-bilayer films, and high permeabilities will allow the use of thicker membranes to increase capacity. Chapter 3 discusses the performance of modified membranes in binding negatively and positively charged particles. Nylon membranes modified with 3 bilayers of PSS/PEI have a Au-colloid binding capacity of 37±6 mg/mL at 80% breakthrough, whereas membranes modified with PSS-terminated films serve as cation-exchange membranes that exhibit a lysozyme binding capacity of 16 mg/mL at 80% breakthrough. A stack of three membranes has a binding capacity equivalent to the sum of the capacities of three individual membranes.

4.2 Future Work

Although the binding performance of ion-exchange membranes prepared by LBL polyelectrolyte adsorption is competitive with that of commercial membrane absorbers, the elution of bound protein from the polyelectrolyte films remains an issue. I attempted protein elution with several common eluents but recovered less than 2% of the bound lysozyme. The low recovery likely stems from multiple interactions between the protein and the polyelectrolytes. Still, perhaps other elution procedures would be effective, and the elution of proteins that are not as highly charged as lysozyme may be much easier. Future work is needed in this area.

This thesis only discusses the binding of Au colloids and lysozyme to these ion-exchange membranes. Husson and coworkers demonstrated successful binding of BSA (a negatively charged protein at neutral pH) to their anion-exchange membranes,[1, 2] and Bhattacharyya and colleagues examined the binding of catalytic enzymes to polyelectrolyte-functionalized polymeric membranes.[3] Furthermore, membrane absorbers are very attractive in the areas of virus capture,[4] vector extraction,[5] and DNA purification.[6] Adsorption of all of these types of analytes could be the subject of future studies with our ion-exchange membranes. Importantly, virus removal requires extremely high capture efficiencies, but elution is not necessary in many cases. The polyelectrolyte membranes may be particularly attractive in this regard if elution is problematic.

4.3 References

1. Bhut, B. V.; Wickramasinghe, S. R.; Husson, S. M., Preparation of High-Capacity, Weak Anion-Exchange Membranes for Protein Separations Using Surface-Initiated Atom Transfer Radical Polymerization. *Journal of Membrane Science* **2008,** 325, (1), 176-183.

2. Bhut, B. V.; Husson, S. M., Dramatic Performance Improvement of Weak Anion-Exchange Membranes for Chromatographic Bioseparations. *Journal of Membrane Science* **2009,** 337, (1-2), 215-223.

3. Datta, S.; Cecil, C.; Bhattacharyya, D., Functionalized Membranes by Layer-by-Layer Assembly of Polyelectrolytes and in Situ Polymerization of Acrylic Acid for Applications in Enzymatic Catalysis. *Industrial & Engineering Chemistry Research* **2008,** 47, (14), 4586-4597.

4. Lars, O.; Sylvia, L.; Udo, R.; Michael, W. W., Sulfated Membrane Adsorbers for Economic Pseudo-Affinity Capture of Influenza Virus Particles. *Biotechnology and Bioengineering* **2009,** 103, (6), 1144-1154.

5. Cristina, P.; Tiago, B. F.; Marcos, F. Q. S.; Manuel, J. T. C.; Paula, M. A., Towards Purification of Adenoviral Vectors Based on Membrane Technology. *Biotechnology Progress* **2008,** 24, (6), 1290-1296.

6. Guerrero-Germán, P.; Prazeres, D.; Guzmán, R.; Montesinos-Cisneros, R.; Tejeda-Mansir, A., Purification of Plasmid DNA Using Tangential Flow Filtration and Tandem Anion-Exchange Membrane Chromatography. *Bioprocess and Biosystems Engineering* **2009,** 32, (5), 615-623.